Received: 10 June 2022 | Revised: 23 January 2023 | Accepted: 24 January 2023

DOI: 10.1002/nme.7214

RESEARCH ARTICLE

WILEY

Multigrid for the dual formulation of the frictionless Signorini problem

Gabriele Rovi[1] | **Bernhard Kober**[2] | **Gerhard Starke**[2] | **Rolf Krause**[1]

[1]Euler Institute, Università della Svizzera Italiana, Lugano, Switzerland

[2]Universität Duisburg-Essen, Forschungsgebiet Numerische Mathematik und Wissenschaftliches Rechnen, Arbeitsgruppe Numerische Mathematik, Essen, Germany

Correspondence
Gabriele Rovi, Euler Institute, Università della Svizzera Italiana, Via Giuseppe Buffi 13, 6900 Lugano, Switzerland.
Email: gabriele.rovi@usi.ch

Funding information
Deutsche Forschungsgemeinschaft (DFG), Grant/Award Number: 186407; Swiss National Science Foundation

Abstract

We examine the dual formulation of the frictionless Signorini problem for a deformable body in contact with a rigid obstacle. We discretize the problem by means of the finite element method. Since the dual formulation solves directly for the stress variable and is not affected by locking, it is very attractive for many engineering applications. However, it is hard to solve it efficiently, since many challenges arise. First, the stress belongs to the non-Sobolev space $\mathbf{H}_{\mathrm{div}}$. Second, the matrix block related to the stress is only semi-positive definite in the incompressible limit. Third, global equality constraints and box-constraints are enforced. In this paper, we propose a novel and optimal nonlinear multigrid method for the dual formulation of the Signorini problem, that works even in the incompressible limit. We opt for the combination of a truncation of the basis functions strategy and a nonlinear monolithic patch smoother with Robin conditions of parameter α. Numerical experiments show that multigrid performance is recovered if α is chosen properly. We propose an algorithm to dynamically update the parameter α during the multigrid process, in order to provide a near optimal value of α.

KEYWORDS

nonlinear, multigrid, dual Signorini problem, incompressibility, Robin conditions

1 | INTRODUCTION

In contact problems, the body of interest, subject to external displacements and forces, cannot penetrate a given obstacle. We assume the main body to be deformable and the obstacle to be rigid. This kind of setting is called Signorini problem. In this paper, we neglect friction and therefore we only focus on the frictionless Signorini problem. We refer the reader to Reference 1 for further reading on this topic.

In many engineering contact problems, it is necessary to deal with nearly-incompressible or incompressible materials and to have a good approximation of the internal stresses. For example, a building is structure composed by many parts that come into contact and that can be assumed to be nearly-incompressible or even incompressible. To determine if the project of the building satisfies the standard or not, usually the internal stresses generated by the deformation have to be computed. Therefore, it can be useful to apply a formulation that describes the Signorini problem for nearly incompressible and incompressible materials and that gives direct access to the stress.

The physical unknowns of the strong form of the Signorini problem are the displacement $\mathbf{u}$ and the stress $\boldsymbol{\sigma}$. However, when it comes to the weak formulations, typically only one of the two variables is the unknown, while the other one has to be postprocessed. For example, the primal weak form solves for the only displacement $\mathbf{u} \in \mathbf{H}_1$ and computes the stress $\boldsymbol{\sigma}$ by differentiation of the displacement. Furthermore, it is affected by locking, thus it cannot easily handle nearly-incompressible or incompressible materials. On the other hand, the dual formulation directly computes the stress $\boldsymbol{\sigma} \in \mathbf{H}_{\text{div}}$. To this purpose, the conservation of linear and angular momenta has to be enforced using the Lagrange multipliers $\mathbf{u}$ and $\boldsymbol{\theta}$ and an LBB (Ladyzhenskaya–Babuška-Brezzi) condition must be satisfied. The main advantages of the dual formulation are twofold. First, it can deal with nearly incompressible and incompressible materials with no additional effort. Second, the dual formulation does not have to postprocess the stress. For these reasons, in this paper, we examine the dual formulation for the frictionless Signorini problem, that we discretize by means of the finite element (FE) method. To satisfy the discrete LBB condition, we use the first-order Raviart–Thomas elements for the stress $\boldsymbol{\sigma}$, while for $\mathbf{u}$ and $\boldsymbol{\theta}$ we, respectively, use discontinuous linear Lagrangian elements and skew-symmetric continuous linear Lagrangian tensors. We refer the reader to Reference 2 for further details on this choice. For the sake of simplicity, only homogeneous and isotropic materials will be examined. Our aim is to design a novel optimal multigrid method (MGM) for the discretized weak form of the dual frictionless Signorini problem. Our method can be interpreted as a combination of a MGM with smoothing property and an inexact active set strategy. To the authors' knowledge, an optimal solver for this problem has not been proposed yet.

MGMs are iterative solvers that aim for optimal complexity—the convergence rate is independent of the dimension of the problem. However, in case of contact mechanics, it is challenging to define an optimal MGM. Indeed, the presence of the obstacle introduces a nonlinearity into the problem. Such nonlinearity, in the primal and in the dual formulations, can be expressed in terms of box-constraints. In order to maintain optimal complexity, a MGM for the Signorini problem has to directly tackle the nonlinearity at each iteration. The primal formulation of the frictionless Signorini problem can be interpreted as the minimization problem of a quadratic functional on a closed convex set, where box-constraints are enforced. The monotone multigrid for this formulation is a nonlinear multigrid with optimal complexity. The main idea is to sequentially minimize the energy functional by means of fine and coarse local corrections that satisfy the fine constraints. Global convergence is ensured on the fine level by using, as a smoother, the projected Gauss–Seidel method. On the coarser levels, the same smoother can be used. However, to ensure that it satisfies the fine constraints, monotone restriction operators are used on the box-constraints. To accelerate the overall process, a truncation strategy of the basis functions is carried out. For other details on this topic, see References 3-11. However, the only primal case is investigated by these papers.

In contrast to the primal formulation of the Signorini problem, the dual formulation is also subject to global equality constraints. They could be directly applied on the coarser problems, but would be redundant and make the method suboptimal. Instead, we project them on the coarser levels, as done in Reference 12. However, since the fine global constraints cannot be satisfied anymore on the coarser levels, we cannot ensure sequential energy minimization. For this reason, we can also avoid to use the monotone restrictions operators for the box-constraints and solve for linear coarse problems. Even though the energy cannot be sequentially minimized, we can still exploit two main ideas of the monotone MGM: the resolution of box-constraints at the fine level and the truncation of the basis functions. In this way, we would still be able to encorporate the nonlinearity at the fine and at the coarser levels.

To fulfill the box-constraints on the fine level, we could use the standard projected Gauss-Seidel method, that acts on mono-dimensional subspaces. However, this smoother is not able to handle the issues explained in Reference 12. First, the stress variable $\boldsymbol{\sigma}$ belongs to the non-Sobolev space $\mathbf{H}_{\text{div}}$ and divergence-free components of the error have to be properly smoothed. Second, in the incompressible limit, the bilinear form related to the stress variable is only semi-positive definite and thus it is not invertible. Third, the global equality constraints have to be fulfilled. All these features are solved by the monolithic patch smoother with Robin boundary conditions of parameter α, introduced in Reference 12 for the dual formulation of linear elasticity. In addition, a fourth difficulty has to be taken into account: the box-constraints. Therefore, on the fine level, we consider a monolithic patch smoother that solves for local corrections that satisfy the box-constraints and that fulfill local Robin boundary conditions. On coarser levels, we only project the global equality constraints but not the box-constraints, so we can reuse the linear monolithic patch smoother of Reference 12. As we will see, even though the coarser problems are linear, the nonlinear information at the fine level is transferred to the coarser levels by means of the truncation strategy. By gluing all these ingredients, we recover a nonlinear MGM for the dual formulation of the frictionless Signorini problem that works even in the incompressible limit.

In Section 2, we introduce the strong formulation of the frictionless Signorini problem for a homogeneous and isotropic body. Here, we discuss the choice of the constitutive law to describe also nearly incompressible and incompressible materials. In Section 3, the dual formulation of the Signorini problem is presented as a minimization problem. In Section 4, we use the finite-element method to discretize it. Thanks to a local orthogonal transformation, the nonlinearity reduces to box-constraints. In order to solve the problem, we design a MGM in Section 5. We discuss its main ingredients, the truncation and the smoother, and the algorithms, respectively in Sections 5.1,5.2, and 5.3. In Section 6, we present numerical experiments for the proposed MGM. Since the smoother enforces local Robin boundary conditions of parameter α, the simulations are carried out for different values of this parameter. We recover optimality of the method for specific values of α, that unfortunately are not known in advance. For this reason, in Section 6.3, we propose a very simple algorithm to dynamically update the value of α_k at each multigrid iteration k. If the initial value α_0 is chosen sufficiently large and smaller than one, then we recover optimality.

2 | THE STRONG FORMULATION OF THE FRICTIONLESS SIGNORINI PROBLEM

In this section, we examine the strong formulation of the frictionless Signorini problem for a homogeneous and isotropic body that can come into contact with a rigid obstacle. With respect to the linear elastic case presented in Reference 12, we must take into account also the contact conditions, prescribed on the surface of the contact boundary. For this reason, we first recall the volumetric equations, that are the same as for the linear elastic case, and then discuss the ones on the boundary.

Let $\Omega \subset \mathbb{R}^d$, for $d = 2, 3$, be the domain of an elastic body, subject to the external volumetric force $\mathbf{f} : \Omega \to \mathbb{R}^d$ on Ω. The conservation of linear and angular momenta of the body Ω are given by the following relations:

$$\operatorname{div} \boldsymbol{\sigma} = -\mathbf{f} \qquad \text{in } \Omega, \tag{1a}$$

$$\mathbf{skw}\, \boldsymbol{\sigma} = \mathbf{0} \qquad \text{in } \Omega, \tag{1b}$$

where we define the skew-symmetric part of the stress $\boldsymbol{\sigma}$ as:

$$\mathbf{skw}\boldsymbol{\sigma} := \frac{1}{2}(\boldsymbol{\sigma} - \boldsymbol{\sigma}^T). \tag{2}$$

We assume the strain $\boldsymbol{\varepsilon}$ to be small enough, so that the kinematic relation between the strain $\boldsymbol{\varepsilon}$ and displacement $\mathbf{u}$ is linear:

$$\boldsymbol{\varepsilon}(\mathbf{u}) := \frac{1}{2}\left(\nabla \mathbf{u} + (\nabla \mathbf{u})^T\right). \tag{3}$$

We also assume the body to be homogeneous and isotropic, subject to a linear constitutive law. In particular, we consider the strain $\boldsymbol{\varepsilon}$ as a function of the stress $\boldsymbol{\sigma}$:

$$\boldsymbol{\varepsilon} = \mathcal{A}\boldsymbol{\sigma} := \frac{1}{2\mu}\left(\boldsymbol{\sigma} - \frac{\lambda}{d\lambda + 2\mu}(\operatorname{tr}\boldsymbol{\sigma})\mathbf{I}\right), \tag{4}$$

where $\mathcal{A}$ is the *compliance tensor*, μ and λ are the Lamé parameters, $\mathbf{I}$ is the identity matrix in d-dimension and $\operatorname{tr} : \mathbb{R}^{d,d} \to \mathbb{R}$, defined such that $\operatorname{tr}(\cdot) := \sum_{i=1}^{d} [\cdot]_{ii}$, is the trace operator.

The body's surface $\partial\Omega$ is divided into three disjoint open sets, the Neumann boundary Γ_N, the Dirichlet boundary Γ_D and the contact boundary Γ_C, so that $\overline{\partial\Omega} = \overline{\Gamma}_D \cup \overline{\Gamma}_N \cup \overline{\Gamma}_C$ and $\Gamma_i \cap \Gamma_j = \emptyset$, for $i, j = C, D, N$ and $i \neq j$. Furthermore, we assume Γ_C to be surrounded by Γ_N. We prescribe the force $\mathbf{g}_N : \Gamma_N \to \mathbb{R}^d$ on Γ_N and the displacement $\mathbf{g}_D$ on Γ_D. The corresponding Neumann and Dirichlet boundary conditions are the following:

$$\boldsymbol{\sigma}\mathbf{n} = \mathbf{g}_N \qquad \text{on } \Gamma_N, \tag{5a}$$

$$\mathbf{u} = \mathbf{g}_D \qquad \text{on } \Gamma_D, \tag{5b}$$

where $\mathbf{n}$ represents the outward normal of the boundary $\partial\Omega$. In order to close the problem, the contact conditions must be enforced on Γ_C. Let us denote with g the distance in the normal direction between Γ_C and the rigid obstacle. We denote with the subscripts n and t the normal and tangential components. So, we define $u_n := \mathbf{u}\cdot\mathbf{n}$, $\sigma_n = \mathbf{n}^T\cdot(\boldsymbol{\sigma}\mathbf{n})$ and $(\boldsymbol{\sigma}\mathbf{n})_t := \boldsymbol{\sigma}\mathbf{n} - \sigma_n\mathbf{n}$. Then the frictionless contact conditions read as follows:

$$g - u_n \le 0 \quad \text{on } \Gamma_C, \tag{6a}$$
$$\sigma_n \le 0 \quad \text{on } \Gamma_C, \tag{6b}$$
$$\sigma_n(g - u_n) = 0 \quad \text{on } \Gamma_C, \tag{6c}$$
$$(\boldsymbol{\sigma}\mathbf{n})_t = \mathbf{0} \quad \text{on } \Gamma_C. \tag{6d}$$

The first inequality (6a) implies that the body Ω can never penetrate the obstacle and for this reason it is called *nonpenetration condition*. The second inequality (6b) states that, in case of contact, only negative pressure is permitted and no adhesion force can occur. The third equation (6c) is referred as *complementarity condition*. It says that the body can be subject to an external pressure only if it is in contact with the obstacle. The last equation (6d) is known as frictionless condition: we assume that no friction force can arise during the contact process. Therefore we seek for sufficiently smooth displacements $\mathbf{u} : \Omega \to \mathbb{R}^d$ and internal stresses $\boldsymbol{\sigma} : \Omega \to \mathbb{R}^{d,d}$ that solve the Signorini problem, given by (1), (4), (5), (6).

Remark 1. In the constitutive law (4), the strain $\boldsymbol{\epsilon}$ remains bounded even in the incompressible limit $\lambda \to \infty$. Thus, a formulation that exploits this kind of relation can easily deal with incompressible and nearly incompressible materials. This is the case of the dual formulation that will be introduced in the next section. On the other hand, the primal formulation typically uses the Hooke's law:

$$\boldsymbol{\sigma} = C\boldsymbol{\epsilon} := 2\mu\boldsymbol{\epsilon} + \lambda(\mathrm{tr}(\boldsymbol{\epsilon}))\mathbf{I}, \tag{7}$$

in which the stress $\boldsymbol{\sigma}$ is expressed as a function of the strain $\boldsymbol{\epsilon}$ by means of the *stiffness tensor* C. Since the constitutive law (7) is not bounded anymore for any entry, locking phenomena arise and it is more challenging to consider incompressible and nearly incompressible bodies for the primal formulation.

3 | THE DUAL FORMULATION OF THE FRICTIONLESS SIGNORINI PROBLEM

We define the following sets:

$$H_{\mathrm{div}}(\Omega) := \{\boldsymbol{\sigma} \in \mathbf{L}^2(\Omega) : \mathrm{div}\boldsymbol{\sigma} \in L^2(\Omega)\}, \tag{8a}$$
$$\boldsymbol{\Sigma} := \{\boldsymbol{\sigma} \in [H_{\mathrm{div}}(\Omega)]^d\}, \tag{8b}$$
$$\boldsymbol{\Sigma}_t := \{\boldsymbol{\sigma} \in [H_{\mathrm{div}}(\Omega)]^d : \boldsymbol{\sigma}\mathbf{n}|_{\Gamma_N} = \mathbf{g}_N,\ (\boldsymbol{\sigma}\mathbf{n})_t|_{\Gamma_C} = \mathbf{0}\}. \tag{8c}$$
$$\mathbf{U} := \left[L^2(\Omega)\right]^d, \tag{8d}$$
$$\boldsymbol{\Theta} := \{\boldsymbol{\gamma} \in \left[L^2(\Omega)\right]^{d,d} : \boldsymbol{\gamma} + \boldsymbol{\gamma}^T = \mathbf{0}\}, \tag{8e}$$

where the space $\boldsymbol{\Sigma}_t$ encorporates the Neumann conditions and the frictionless contact conditions. Furthermore, the bilinear and linear forms of the problem are the following:

$$a(\boldsymbol{\sigma}, \boldsymbol{\tau}) := \int_\Omega \mathcal{A}\boldsymbol{\sigma} : \boldsymbol{\tau}, \tag{9a}$$
$$b(\boldsymbol{\sigma}, \mathbf{u}) := \int_\Omega \mathbf{u}\cdot\mathrm{div}\boldsymbol{\sigma}, \tag{9b}$$
$$c(\boldsymbol{\sigma}, \boldsymbol{\theta}) := \int_\Omega \boldsymbol{\theta} : \mathbf{skw}(\boldsymbol{\sigma}), \tag{9c}$$
$$f_a(\boldsymbol{\sigma}) := \int_{\Gamma_D} \boldsymbol{\sigma}\mathbf{n}\cdot\mathbf{g}_D + \int_{\Gamma_C} \sigma_n\, g, \tag{9d}$$
$$f_b(\mathbf{v}) := -\int_\Omega \mathbf{f}\cdot\mathbf{v}. \tag{9e}$$

The Signorini problem can be formulated as the minimization of the quadratic functional $\mathcal{J} : \mathbf{\Sigma} \to \mathbb{R}$ over the nonempty closed convex set $\mathbf{K}$:

$$\mathcal{J}(\boldsymbol{\sigma}) := \frac{1}{2}a(\boldsymbol{\sigma},\boldsymbol{\sigma}) - f_a(\boldsymbol{\sigma}), \tag{10a}$$

$$\begin{aligned}\mathbf{K} := \{\boldsymbol{\sigma} \in \mathbf{\Sigma}_t : \; & b(\boldsymbol{\sigma},\mathbf{v}) = f_b(\mathbf{v}) && \forall \mathbf{v} \in \mathbf{U},\\ & c(\boldsymbol{\sigma},\boldsymbol{\gamma}) = 0 && \forall \boldsymbol{\gamma} \in \mathbf{\Theta},\\ & \sigma_n \le 0 && \text{on } \Gamma_C\}.\end{aligned} \tag{10b}$$

The equality constraints $\operatorname{div} \boldsymbol{\sigma} = -\mathbf{f}$ and $\mathbf{skw}\boldsymbol{\sigma} = \mathbf{0}$ are written weakly in (10b) and can be, respectively, enforced by the Lagrange multipliers, $\mathbf{u} \in \mathbf{U}$ and $\boldsymbol{\theta} \in \mathbf{\Theta}$. The closed convex set $\mathbf{K}$ is nonempty due to the fulfilment of an LBB condition. In Reference 2, it is proven that there exists $\beta > 0$ such that:

$$\inf_{\mathbf{u}\mathbf{U}\in\boldsymbol{\theta}\in\mathbf{\Theta}} \sup_{\boldsymbol{\sigma}\mathbf{\Sigma}\in} \frac{b(\boldsymbol{\sigma},\mathbf{u}) + c(\boldsymbol{\sigma},\boldsymbol{\theta})}{\|\boldsymbol{\sigma}\|_{\mathbf{\Sigma}}(\|\mathbf{u}\|_{\mathbf{U}} + \|\boldsymbol{\theta}\|_{\mathbf{\Theta}})} \ge \beta > 0. \tag{11}$$

Then the solution $\hat{\boldsymbol{\sigma}}$ is the minimizer $\hat{\boldsymbol{\sigma}} = \operatorname{argmin}_{\boldsymbol{\sigma}\in\mathbf{K}}\mathcal{J}(\boldsymbol{\sigma})$. For further details on the formulation and the existence and uniqueness of the solution of the Signorini problem, see.[13]

4 | MIXED DISCRETIZATION

Let $\mathcal{T}_h = \{K_1, \dots, K_{N_e}\}$ be a shape-regular simplicial mesh of Ω with N_e elements. The element K is a simplex in d dimension: a triangle for $d = 2$, a tetrahedron for $d = 3$. The subscript h represents the maximal diameter of $\mathcal{T}_h$. We discretize the continuous spaces $\mathbf{\Sigma}$, $\mathbf{U}$ and $\mathbf{\Theta}$ on the mesh $\mathcal{T}_h$ by means of the finite element method. We get $\mathbf{\Sigma}_h$, $\mathbf{U}_h$ and $\mathbf{\Theta}_h$. The discretization of all the other known functions, such as $\mathbf{n}$, $\mathbf{f}$, $\mathbf{g}_D$, $\mathbf{g}_N$, g, gives rise to $\mathbf{n}_h$, $\mathbf{f}_h$, $\mathbf{g}_{h,D}$, $\mathbf{g}_{h,N}$, g_h. The discretized bilinear and linear forms in (9) are denoted with the subscript h. The discrete bilinear forms (9b) and (9c) must satisfy the discrete version of the LBB condition (11). To this purpose, the discrete spaces must be chosen properly. We opt for the same triplet as in References 2,12,13:

$$\mathbf{\Sigma}_h = \left[RT_1(\mathcal{T}_h)\right]^d, \tag{12a}$$

$$\mathbf{U}_h = \left[DP_1(\mathcal{T}_h)\right]^d, \tag{12b}$$

$$\mathbf{\Theta}_h = \left[P_1(\mathcal{T}_h)\right]^{d\times d} \cap \mathbf{\Theta}, \tag{12c}$$

where RT_1, P_1, and DP_1 are, respectively, the spaces of first-order Raviart–Thomas, continuous linear Lagrangian and discontinuous linear Lagrangian functions. See References 2,14. We seek for $\boldsymbol{\sigma}_h \in \mathbf{\Sigma}_{t,h}$ such that it minimizes the functional $\mathcal{J}_h$ over the closed convex set $\mathbf{K}_h$:

$$\mathcal{J}_h(\boldsymbol{\sigma}_h) := \frac{1}{2}a_h(\boldsymbol{\sigma}_h,\boldsymbol{\sigma}_h) - f_{a,h}(\boldsymbol{\sigma}_h), \tag{13a}$$

$$\begin{aligned}\mathbf{K}_h := \{\boldsymbol{\sigma}_h \in \mathbf{\Sigma}_{t,h} : \; & b_h(\boldsymbol{\sigma}_h,\mathbf{v}_h) = f_{b,h}(\mathbf{v}_h) && \forall \mathbf{v}_h \in \mathbf{U}_h,\\ & c_h(\boldsymbol{\sigma}_h,\boldsymbol{\gamma}_h) = 0 && \forall \boldsymbol{\gamma}_h \in \mathbf{\Theta}_h,\\ & \sigma_{n,h} \le 0 && \text{on } \Gamma_{C,h}\}.\end{aligned} \tag{13b}$$

Remark 2 (Householder transformation). In general the condition $\sigma_{n,h} \le 0$ in (13b) is not a box constraint. Indeed all the components of the force $\boldsymbol{\sigma}\mathbf{n}$, for $i = 1, \dots, d$, are involved in the single inequality constraint: $(\boldsymbol{\sigma}_h\mathbf{n}_h)\cdot\mathbf{n}_h \le 0$. However, we can change the local coordinate system, by means of an Householder transformation, from Cartesian to an orthogonal coordinate system with first component identified by the direction of the normal $\mathbf{n}$. In this way, only the first component is involved in the inequality $\sigma_{n,h} \le 0$, that becomes a box-constraint in the FE setting. In the following, we assume the formulation (13) to be written by means of local orthogonal transformations.

Once the spaces, their bases and degrees of freedom (dofs) are chosen, it is also possibile to reformulate (13) in a vector-matrix form. Let n and m be the dimensions of the spaces, respectively, of the unknown and of the Lagrange

multipliers related to global constraints, that is, $n = \dim(\mathbf{\Sigma}_h)$ and $m = \dim(\mathbf{U}_h) + \dim(\mathbf{\Theta}_h)$. Furthermore let $\mathbf{y}_h \in \mathbf{Y}_h = \mathbb{R}^n$ and $\mathbf{z}_h \in \mathbf{Z}_h = \mathbb{R}^m$ be the vectors that collect the values of the dofs, respectively, of $\boldsymbol{\sigma}_h$ and $[\mathbf{u}_h, \boldsymbol{\theta}_h]^T$. The problem (13) can be equivalently written in a vector-matrix form. Find $\mathbf{y}_h \in \mathbf{Y}_h$ such that it minimizes $\mathcal{J}_h : \mathbf{Y}_h \to \mathbb{R}$ over the closed convex set $\mathbf{K}_h$:

$$\mathcal{J}_h(\mathbf{y}_h) = \frac{1}{2}\mathbf{y}_h^T\mathbf{A}_h\mathbf{y}_h - \mathbf{y}_h^T\mathbf{f}_h, \tag{14a}$$

$$\mathbf{K}_h = \{\mathbf{y}_h \in \mathbf{Y}_h : \mathbf{B}_h\mathbf{y}_h = \mathbf{h}_h, \quad \mathbf{low}_h \le \mathbf{y}_h \le \mathbf{up}_h\}, \tag{14b}$$

where $\mathbf{A}_h \in \mathbb{R}^{n\times n}$, $\mathbf{B}_h \in \mathbb{R}^{m\times n}$, $\mathbf{f}_h, \mathbf{low}_h, \mathbf{up}_h \in \mathbb{R}^n$ and $\mathbf{h}_h \in \mathbb{R}^m$. The inequalities $\mathbf{low}_h \le \mathbf{y}_h \le \mathbf{up}_h$ are meant component-wise and encorporate both point-wise equality and box-constraints. Indeed the vectors $\mathbf{low}_h, \mathbf{up}_h$ are defined as:

$$[\mathbf{low}_h]_i = \begin{cases} [\mathbf{g}_{N,h}]_i & \text{on } \Gamma_N \\ 0 & \text{on } \Gamma_C \text{ and if the component is tangential} \\ -\infty & \text{otherwise} \end{cases}. \tag{15a}$$

$$[\mathbf{up}_h]_i = \begin{cases} [\mathbf{g}_{N,h}]_i & \text{if on } \Gamma_N \\ 0 & \text{on } \Gamma_C \\ +\infty & \text{otherwise} \end{cases}. \tag{15b}$$

For the sake of simplicity, no Lagrange multiplier is noticeably present in the formulation (14). However, we can explicit all the Lagrange multipliers, by writing the problem in a vector-matrix form. First, we introduce the Lagrangian function:

$$\Lambda_h(\mathbf{y}_h, \mathbf{z}_h, \mathbf{s}_h, \mathbf{t}_h) = \frac{1}{2}\mathbf{y}_h^T\mathbf{A}_h\mathbf{y}_h - \mathbf{z}_h^T(\mathbf{B}_h\mathbf{y}_h - \mathbf{h}_h) - \mathbf{s}_h^T(\mathbf{y}_h - \mathbf{low}_h) - \mathbf{t}_h^T(\mathbf{up}_h - \mathbf{y}_h), \tag{16}$$

where the vectors $\mathbf{z}_h \in \mathbb{R}^m$ and $\mathbf{s}_h, \mathbf{t}_h \in \mathbb{R}^n$ are the Lagrange multipliers, respectively, for the global equality constraints $\mathbf{B}_h\mathbf{y}_h = \mathbf{h}_h$ and the box-constraints $\mathbf{low}_h \le \mathbf{y}_h \le \mathbf{up}_h$. In terms of the KKT (Karush–Kuhn–Tucker) conditions, the problem is rewritten as:

$$\begin{bmatrix} \mathbf{A}_h & \mathbf{B}_h^T \\ \mathbf{B}_h & \mathbf{0} \end{bmatrix} \begin{bmatrix} \mathbf{y}_h \\ \mathbf{z}_h \end{bmatrix} = \begin{bmatrix} \mathbf{f}_h \\ \mathbf{h}_h \end{bmatrix} \tag{17a}$$

$$[\mathbf{y}_h]_i \ge [\mathbf{low}_h]_i \quad i = 1, \dots n \tag{17b}$$

$$[\mathbf{y}_h]_i \le [\mathbf{up}_h]_i, \quad i = 1, \dots n \tag{17c}$$

$$[\mathbf{s}_h]_i \ge 0 \quad i = 1, \dots n \tag{17d}$$

$$[\mathbf{t}_h]_i \ge 0 \quad i = 1, \dots n \tag{17e}$$

$$\mathbf{s}_h^T(\mathbf{y}_h - \mathbf{low}_h) = \mathbf{0} \tag{17f}$$

$$\mathbf{t}_h^T(\mathbf{up}_h - \mathbf{y}_h) = \mathbf{0} \tag{17g}$$

$$\mathbf{z}_h^T(\mathbf{B}_h\mathbf{y}_h - \mathbf{h}_h) = \mathbf{0} \tag{17h}$$

In the nonlinear MGM of Section 5, for the sake of simplicity, we will focus only on the Lagrange multiplier $\mathbf{z}_h$ used to enforce the global constraint $\mathbf{B}_h\mathbf{y}_h = \mathbf{h}_h$ on the fine level and on the coarser levels as well.

Remark 3. In this paper, as done in Reference 12, we rewrite the space $\mathbf{\Theta}_h$ in terms of its components. In particular, for the case $d = 2$, we can write:

$$\mathbf{\Theta}_h = \left\{ \begin{bmatrix} 0 & -p \\ p & 0 \end{bmatrix}, \quad p \in P_1(\mathcal{T}_h) \right\} \quad d = 2, \tag{18}$$

so that we can use only the component p as the new unknown. Thus, the space $\mathbf{\Theta}_h = \left[P_1(\mathcal{T}_h)\right]^{d\times d} \cap \mathbf{\Theta}$ is substituted by $\Theta_h = P_1(\mathcal{T}_h)$.

5 | NONLINEAR MGM

The MGM is an iterative solver that aims for optimal convergence. The single kth iteration of the MGM is called V-Cycle. Then the MGM iterates for $k = 0, 1, \dots, k_{\max}$, with $k_{\max} \in \mathbb{N}$, and at every iteration k a V-Cycle is carried out. If the number of iterations required to get convergence is independent of the dimension of the problem, then the MGM is optimal. For further references, see References 15-20.

A fundamental ingredient of the MGM is the smoother. The smoother is another iterative method that, in few iterations, can damp the high-frequency components of the error. As a stand-alone solver, the smoother performance deteriorates with the increase of the dimension of the problem. However, the MGM exploits the smoothing property by representing the error on different coarser subspaces. In fact, in this way, the low-frequency components become high-frequency components on the coarser subspaces and can be easily smoothed. Therefore, a V-Cycle can be interpreted as the application of few smoothing steps on all the frequencies of the error. Thus, with respect to the only smoother, the overall convergence of the MGM is accelerated and can even produce optimal performances. Therefore, to define a MGM, we require two main ingredients: a hierarchy of nested spaces and the smoother. We first introduce the coarsening process in Section 5.1 and then we examine the smoother in Section 5.2.

For standard linear problems, the MGM is optimal. However, for nonlinear and nonstandard problems, achieving optimality can be more challenging. In this section, we introduce a nonlinear MGM, combined with an inexact active set strategy, for the problem described in (13) and in (14). In particular, we discuss our design choices to achieve optimal convergence. The main difficulties to be faced are the following:

1. $\boldsymbol{\sigma}_h \in [H_{\text{div}}(\Omega)]^d$;
2. The semi-positive definiteness of $\mathbf{A}_h$, in the incompressible limit, $\lambda \to \infty$;
3. The presence of global equality constraints $\mathbf{B}_h\mathbf{y}_h = \mathbf{h}_h$;
4. The nonlinear box-constraint $\sigma_{n,h} \leq 0$;

If $\Gamma_C = \emptyset$, then the Signorini problem boils down to the linear elasticity problem. Then, the MGM has to take into consideration only 1, 2, and 3. A working MGM for this case is proposed in Reference 12. However, if $\Gamma_C \neq \emptyset$, the condition 4 is added to the other ones and a nonlinear problem is recovered. In the nonlinear MGM that we propose, the nonlinearity $\sigma_{n,h} \leq 0$ affects both the coarsening, by means of the truncation of the basis functions discussed in Section 5.1, and the smoother, examined in Section 5.2.

5.1 | Truncation of the basis

Let us introduce a sequence of nested meshes $\{\mathcal{T}_j\}_{j=0}^J$ such that $\mathcal{T}_0 \subset \mathcal{T}_1 \subset \cdots \subset \mathcal{T}_{J-1} \subset \mathcal{T}_J := \mathcal{T}_h$. We can define the following sequences of nested subspaces: $\boldsymbol{\Sigma}_0 \subset \boldsymbol{\Sigma}_1 \subset \cdots \subset \boldsymbol{\Sigma}_{J-1} \subset \boldsymbol{\Sigma}_J := \boldsymbol{\Sigma}_h$, $\mathbf{U}_0 \subset \mathbf{U}_1 \subset \cdots \subset \mathbf{U}_{J-1} \subset \mathbf{U}_J := \mathbf{U}_h$, $\boldsymbol{\Theta}_0 \subset \boldsymbol{\Theta}_1 \subset \dots \subset \boldsymbol{\Theta}_{J-1} \subset \boldsymbol{\Theta}_J := \boldsymbol{\Theta}_h$. Each $\boldsymbol{\Sigma}_j/\mathbf{U}_j/\boldsymbol{\Theta}_j$ is the coarse space on the level j of the space $\boldsymbol{\Sigma}_h/\mathbf{U}_h/\boldsymbol{\Theta}_h$, related to the mesh $\mathcal{T}_j$. For $j = 0, \dots, J$, we can bijectively relate $\boldsymbol{\Sigma}_j$ and $[\mathbf{U}_j, \boldsymbol{\Theta}_j]$ to the spaces of their coefficients, $\mathbf{Y}_j$ and $\mathbf{Z}_j$. For $j = 0, \dots, J-1$, $\boldsymbol{\Pi}_j^{j+1} : \mathbf{Y}_j \to \mathbf{Y}_{j+1}$ and $\mathbf{Q}_j^{j+1} : \mathbf{Z}_j \to \mathbf{Z}_{j+1}$ represent the corresponding interpolation operators between the levels j and $j+1$.

The spaces $\{\mathbf{Y}_j\}_{j=0}^J$ refer to the coefficients of the FE functions belonging to $\{\boldsymbol{\Sigma}_j\}_{j=0}^J$. We can bijectively relate each ith coefficient $[\mathbf{y}_j]_i$ to the ith shape function of the corresponding FE space $\boldsymbol{\Sigma}_j$ on level j. Furthermore, since the hierarchy of the spaces is nested, that is, $\boldsymbol{\Sigma}_0 \subset \cdots \subset \boldsymbol{\Sigma}_J$, the basis functions of the coarse levels, for $j = 0, \dots, J-1$, are built as linear combinations of the basis functions on level J.

At the kth multigrid iteration, the ith dof on level J can become active: $[\mathbf{y}_J^k]_i = [\mathbf{low}_J]_i$ or $[\mathbf{y}_J^k]_i = [\mathbf{up}_J]_i$. We call active set W^k the set of dofs that are active:

$$W^k := \{i \in \mathbb{N} : \quad [\mathbf{y}_J^k]_i = [\mathbf{low}_J]_i \quad \text{or} \quad [\mathbf{y}_J^k]_i = [\mathbf{up}_J]_i\}. \tag{19}$$

We can assume, at least for this iteration, that all the real values $[\mathbf{y}_J^k]_i$, with $i \in W^k$, are known and no further corrections from the coarser spaces are needed in the direction of the corresponding subspaces. We can interpret each dof $i \in W^k$ as subject to a momentary boundary condition, that is, $[\mathbf{y}_J^k]_i = [\mathbf{low}_J]_i$ or $[\mathbf{y}_J^k]_i = [\mathbf{up}_J]_i$. These boundary conditions on the fine level cannot necessarily be represented directly onto the coarser levels. See, for example, Figure 1. However, the *truncation of the fine basis functions* is a way to transfer the information gathered so far in W^k to the coarser levels. It

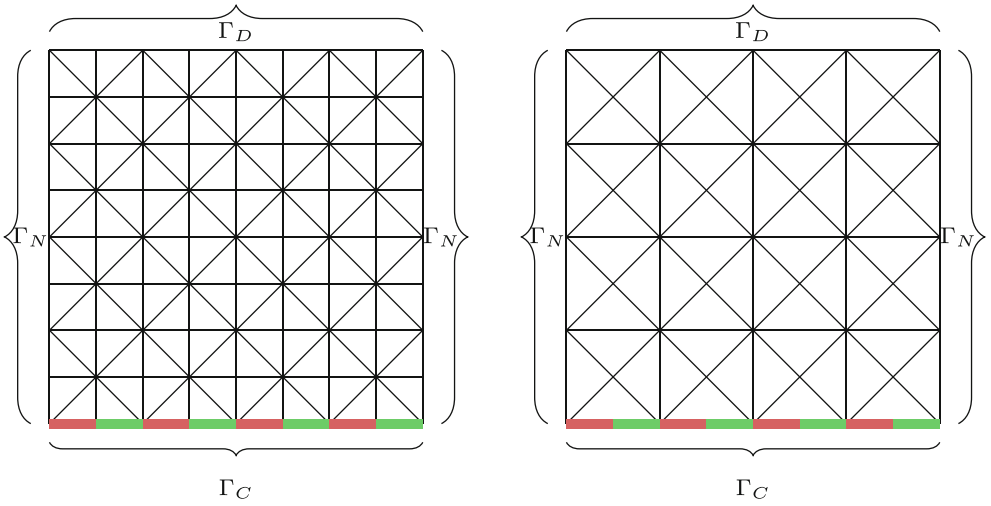

FIGURE 1 On the red edges, we assume the degree of freedoms (dofs) to be active. On the green edges, the dofs are inactive. The fine information cannot be directly represented on the coarse mesh (B).

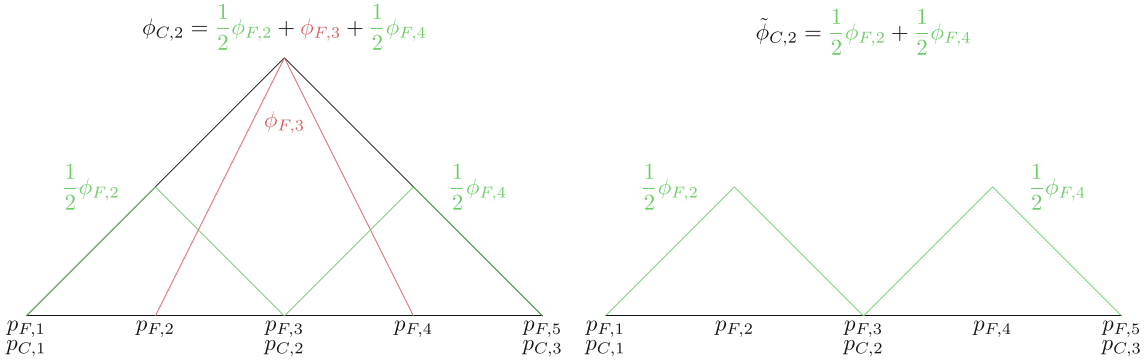

FIGURE 2 The coarse basis function $\phi_{C,2}$ in black is hat function given by the linear combination of $\phi_{F,2}$, $\phi_{F,3}$, $\phi_{F,4}$. If $\phi_{F,3}$ is truncated, the function $\tilde{\phi}_{C,2}$ is now only a linear combination of $\phi_{F,2}$, $\phi_{F,4}$ and no more a hat function.

consists in temporarily removing, for the whole iteration k, all the basis functions on level J corresponding to the dofs in W^k. The coarse basis functions are modified as well, as now they are linear combinations of the *truncated* basis functions on level J. As a consequence, the corrections computed on the coarser levels have no influence on the dofs $i \in W^k$. For further reading on truncation, see again References 3,5. As an example of a truncated shape function for one-dimensional linear Lagrangian elements, see Figure 2. The coarse basis function $\phi_{C,2}$ is a hat function that can be written as $\phi_{C,2} = \frac{1}{2}\phi_{F,2} + \phi_{F,3} + \frac{1}{2}\phi_{F,4}$. If the fine central dof is active, its basis function $\phi_{F,3}$ is removed and $\phi_{C,2}$ is consequently truncated as $\tilde{\phi}_{C,2} = \frac{1}{2}\phi_{F,2} + \frac{1}{2}\phi_{F,4}$ and is no more a hat function.

In terms of implementation, truncation involves the interpolation operator $\mathbf{\Pi}^J_{J-1} : \mathbf{Y}_{J-1} \to \mathbf{Y}_J$. All the rows of $\mathbf{\Pi}^J_{J-1}$ corresponding to the active dofs in W^k are set to zero. We obtain the truncated interpolation operator $\tilde{\mathbf{\Pi}}^J_{J-1}$. Since the box-constraints are considered only at level J, truncation is used only between levels J and $J-1$. Thus, for all other levels $j = 0, \dots, J-2$, the interpolation operators are not changed. We define the operator $\hat{\mathbf{\Pi}}^{j+1}_j$ in (21a) so that these conditions are fulfilled. Then, the coarse problems, for $j = 0, \dots, J-1$, are iteratively defined as:

$$\begin{bmatrix} \mathbf{A}_j & \mathbf{B}_j^T \\ \mathbf{B}_j & \mathbf{0} \end{bmatrix} \begin{bmatrix} \mathbf{y}_j \\ \mathbf{z}_j \end{bmatrix} = \begin{bmatrix} \mathbf{f}_j \\ \mathbf{h}_j \end{bmatrix}, \tag{20}$$

where

$$\hat{\mathbf{\Pi}}_j^{j+1} := \begin{cases} \tilde{\mathbf{\Pi}}_j^{j+1} & j = J-1 \\ \mathbf{\Pi}_j^{j+1} & j = 0, \dots, J-2 \end{cases} \tag{21a}$$

$$\mathbf{A}_j := \left[\hat{\mathbf{\Pi}}_j^{j+1}\right]^T \mathbf{A}_{j+1} \hat{\mathbf{\Pi}}_j^{j+1}, \tag{21b}$$

$$\mathbf{B}_j := \left[\mathbf{Q}_j^{j+1}\right]^T \mathbf{B}_{j+1} \hat{\mathbf{\Pi}}_j^{j+1}, \tag{21c}$$

$$\mathbf{f}_j := \left[\hat{\mathbf{\Pi}}_j^{j+1}\right]^T \left(\mathbf{f}_{j+1} - \mathbf{A}_{j+1}\mathbf{y}_{j+1} - \mathbf{B}_{j+1}^T \mathbf{z}_{j+1}\right), \tag{21d}$$

$$\mathbf{h}_j := \left[\mathbf{Q}_j^{j+1}\right]^T (\mathbf{h}_{j+1} - \mathbf{B}_{j+1}\mathbf{y}_{j+1}). \tag{21e}$$

Each coarse problem (20) at level j depends on the one at level $j+1$ and, recursively, on all the other finer levels. Therefore, the modification of $\mathbf{\Pi}_{J-1}^J$ into $\tilde{\mathbf{\Pi}}_{J-1}^J$ is sufficient to make the fine information on the active dofs travel from level J to level $j = 0$. As an implication, whenever W^k changes, we must repeat the assembly of the coarse matrices $\mathbf{A}_j$ and $\mathbf{B}_j$, for $j = 0, \dots, J-1$. Therefore truncation makes necessary the Galerkin assembly everytime a dof is added or removed from the active set. Dofs related to the essential boundary conditions (5a), (6d), can be considered always active. Thus, the re-assembly of coarse levels is determined only by the box-constraint (6b). Furthermore, we notice that the assembly on coarse levels concern only the dofs related to the boundary Γ_C. Thus, in principle, it is required only a partial assembly of $\mathbf{A}_j$ and $\mathbf{B}_j$, with $j = 0, \dots, J-1$.

Remark 4. In general, the i th coarse basis function on level j can be the linear combination of shape functions on level J all of which have been truncated. If this is the case, the truncated coarse basis function coincides with the zero function. Then the matrix of the saddle point in (20) has no more full rank. Therefore, whenever we compute fine or coarse corrections, we must enforce a zero boundary condition on the corresponding i th dof. In the following, we assume the system (20) for $j = 0$ and the system in Algorithm 2 to be modified accordingly. However, for the sake of simplicity, we will not rewrite the algorithms and we just highlight this fact in this remark.

5.2 | Smoother

The smoother defined in this paper works as a subspace correction method. See Reference 15. In particular, we introduce two different versions: a linear one on the coarser spaces and a nonlinear one for the level J. For each level j, we define the decomposition $\mathbf{Y}_j = \sum_{i=1}^{n_j} \mathbf{Y}_{j,i}$, where each of the n_j subspaces $\mathbf{Y}_{j,i}$ is related to $\mathbf{Y}_j$ by means of the interpolation operator $\mathbf{\Pi}_{j,i} : \mathbf{Y}_{j,i} \to \mathbf{Y}_j$. Similarly we do for $\mathbf{Z}_j = \sum_{i=1}^{n_j} \mathbf{Z}_{j,i}$, with the interpolation $\mathbf{Q}_{j,i} : \mathbf{Z}_{j,i} \to \mathbf{Z}_j$. Then the smoother must solve for local problems on these subspaces. We need to determine the support of these subspace, so that certain requirements are fulfilled.

As a linear smoother, we use the same discussed in Reference 12, where a MGM for the dual weak form of the linear elasticity problem is presented. The nonlinear smoother for the level J is defined as the one in Reference 12, but it solves for local constrained optimization problems. To define a smoother of this kind, the following main difficulties have to be tackled:

- The error components related to the stress $\boldsymbol{\sigma} \in [H_{\text{div}}(\Omega)]^d$ cannot be smoothed with standard Gauss–Seidel, that sequentially acts on one-dimensional subspaces. Indeed, divergence-free components must be tackled by means of a patch smoother, like the Arnold-Falk-Winther smoother, that computes corrections on larger subspaces. See References 21-23. In Figure 3, we represent the patch subspace for the only stress variable. Since the problem is d-dimensional, each green circle represents the d-dof components of the stress. The Lagrange multipliers, the red triangles for the displacement and the blue circles for the rotation, are not present.
- In the incompressible limit, for $\lambda \to \infty$, the matrix $\mathbf{A}_h$ becomes only semi-positive definite and thus it is not invertible. However, since the LBB condition is fulfilled, the whole system (22) is invertible:

$$\begin{bmatrix} \mathbf{A}_h & \mathbf{B}_h^T \\ \mathbf{B}_h & \mathbf{0} \end{bmatrix} \begin{bmatrix} \mathbf{y}_h \\ \mathbf{z}_h \end{bmatrix} = \begin{bmatrix} \mathbf{f}_h \\ \mathbf{h}_h \end{bmatrix}. \tag{22}$$

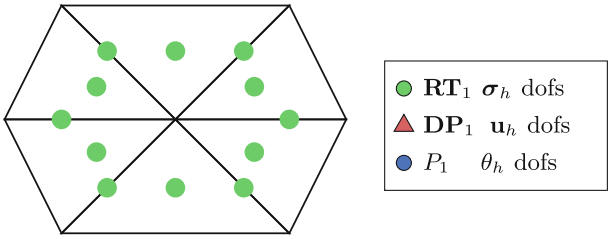

FIGURE 3 Patch subspace for tackling divergence-free components of the stress. Only the green stress degrees of freedom (dofs), $\boldsymbol{\sigma}_h \in \boldsymbol{RT}_1$, are present. No global equality constraint and thus no Lagrange multiplier, $\mathbf{u}_h \in \mathbf{P}_1$ and $\theta_h \in \mathrm{P}_1$, is considered. The figure is presented also in Reference 12.

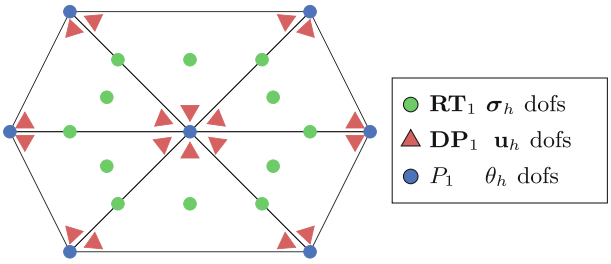

FIGURE 4 Subspace related to a patch with Neumann boundary conditions. The LBB condition is satisfied. The figure is presented also in Reference 12.

For this reason, a *monolithic patch* smoother that takes into account altogether the main unknown $\mathbf{y}_h$ and the Lagrange multipliers $\mathbf{z}_h$ must be considered. Otherwise, even locally, the subproblem does not satisfy the LBB condition and cannot be well-posed. However, if we take into account only the internal stress dofs, a pure Neumann boundary condition is enforced on the patch boundary. In this way, the subproblem is still not well-posed, see Figure 4.

- To get convergence of the whole smoothing process, stress components must be considered also on the boundary of the patch. In particular, to increase the overall performance, Robin boundary conditions of parameter $\alpha \geq 0$ can be enforced. The Robin boundary conditions must be enforced only for dofs that lie on the boundary of the patch that, however, is not part of the boundary of the mesh. Indeed the parameter α is used to enhance the overall communication process among patches. The effect of these conditions is to damp the components of the stress correction on the boundary, so that, locally, the global equality constraints ($\mathbf{B}_h\mathbf{y}_h = \mathbf{h}_h$) are violated in a minor way. For details, see Reference 12.
- Since the box-constraint $\sigma_{n,h} \leq 0$ has to be fulfilled on Γ_C, on the fine level J, the smoother must solve local constrained optimization problems. Boundary dofs satisfying $\sigma_{n,h} \leq 0$ lie on the mesh boundary, so they are not subject to the local Robin boundary conditions. The same happens for all the dofs belonging to the boundary, where no communication with other patches is required.

The subspace of a patch smoother, that takes into account all the ingredients introduced above, is represented in Figure 5. An iterative subspaces correction method of this kind is a monolithic patch smoother with local Robin boundary conditions. Then it can be linear or nonlinear, depending on the nature of the local subproblem.

Once the subspaces are defined, the local matrices and vectors, for $j = 0, \ldots, J$, can be defined as follows:

$$\mathbf{A}_{j,i} := \mathbf{\Pi}_{j,i}^T \mathbf{A}_j \mathbf{\Pi}_{j,i}, \tag{23a}$$

$$\mathbf{B}_{j,i} := \mathbf{Q}_{j,i}^T \mathbf{B}_j \mathbf{\Pi}_{j,i}, \tag{23b}$$

$$\mathbf{f}_{j,i} := \mathbf{\Pi}_{j,i}^T \left(\mathbf{f}_j - \mathbf{A}_j \mathbf{y}_j - \mathbf{B}_j^T \mathbf{z}_j \right), \tag{23c}$$

$$\mathbf{h}_{j,i} := \mathbf{Q}_{j,i}^T (\mathbf{h}_j - \mathbf{B}_j \mathbf{y}_j), \tag{23d}$$

while, for $j = J$, the local box-constraints are:

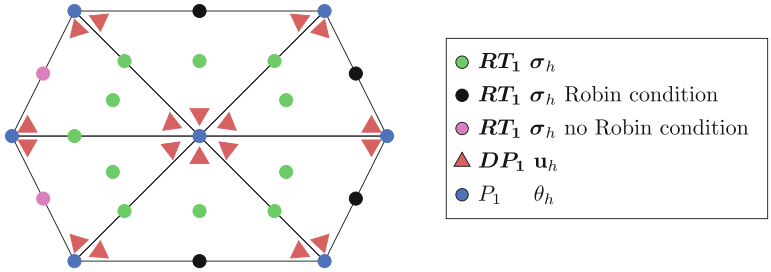

FIGURE 5 Subspace referred to a patch where local Robin boundary conditions are enforced on the portion of the boundary patch that is not a subset of the mesh boundary. The purple stress dofs lie on the boundary of the mesh corresponding to Γ_C, Γ_D, or Γ_N. The black dofs are related to stress dofs that communicate with other patches. For simplicity, each circle and triangle represents all the dofs components of the given quantity.

$$\mathbf{low}_{J,i} = \mathbf{low}_J - \mathbf{y}_J, \tag{24a}$$

$$\mathbf{up}_{J,i} = \mathbf{up}_J - \mathbf{y}_J. \tag{24b}$$

The dofs related to the subspace $\mathbf{Y}_{j,i}$ can be distinguished between internal and boundary dofs, respectively, denoted with the subscripts "int" and "ext." On the external dofs, local discrete Robin boundary conditions of parameter $\alpha \geq 0$ are applied. We remind that the external dofs are the ones on the boundary patch that are not on the boundary mesh. Indeed, the Robin conditions are used to improve the global communication process among patches. If a dof is not common between two or more patches, then no communication has to be improved. We introduce a diagonal matrix $\mathbf{G} = \mathbf{G}(\alpha)$:

$$[\mathbf{G}(\alpha)]_{p,q} = \begin{cases} \alpha \max_s \max\left(|(\mathbf{A}_{\text{ext,ext}})_{p,s}|, |(\mathbf{A}^T_{\text{int,ext}})_{p,s}|, |(\mathbf{B}^T_{\text{int,ext}})_{p,s}| \right) & p = q \\ 0 & p \neq q \end{cases}, \tag{25}$$

and the new matrix $\hat{\mathbf{A}}_{j,i}$ that takes into account also the discrete Robin conditions:

$$\hat{\mathbf{A}}_{j,i} = \begin{bmatrix} \mathbf{A}_{\text{ext,ext}} + \mathbf{G}(\alpha) & \mathbf{A}^T_{\text{int,ext}} \\ \mathbf{A}_{\text{int,ext}} & \mathbf{A}_{\text{int,int}} \end{bmatrix}. \tag{26}$$

The subproblem on the fine level J and related to the ith subspace is the following: find $\mathbf{y}_{j,i}$ and $\mathbf{z}_{j,i}$ so that the following problem is minimized:

$$\mathcal{J}_{j,i}(\mathbf{y}_{j,i}) = \frac{1}{2}\mathbf{y}^T_{j,i}\hat{\mathbf{A}}_h\mathbf{y}_{j,i} - \mathbf{y}^T_{j,i}\mathbf{f}_h \ :, \tag{27a}$$

$$\mathbf{K}_{j,i} = \{\mathbf{y}_{j,i} \ : \ \mathbf{B}_{j,i}\mathbf{y}_{j,i} = \mathbf{h}_{j,i}, \quad \mathbf{low}_{j,i} \leq \mathbf{y}_{j,i} \leq \mathbf{up}_{j,i}\}, \tag{27b}$$

where $\mathbf{z}_{j,i}$ represents the Lagrange multiplier vector used in the KKT condition to enforce $\mathbf{B}_{j,i}\mathbf{y}_{j,i} = \mathbf{h}_{j,i}$. On the other hand, for $j = 0, \ldots, J-1$, the local subproblems can be written as saddle point systems: find $\mathbf{y}_{j,i}$ and $\mathbf{z}_{j,i}$ that solve the following system:

$$\begin{bmatrix} \hat{\mathbf{A}}_{j,i} & \mathbf{B}^T_{j,i} \\ \mathbf{B}_{j,i} & \mathbf{0} \end{bmatrix} \begin{bmatrix} \mathbf{y}_{j,i} \\ \mathbf{z}_{j,i} \end{bmatrix} = \begin{bmatrix} \mathbf{f}_{j,i} \\ \mathbf{h}_{j,i} \end{bmatrix}, \tag{28}$$

5.3 | MGM algorithm

The algorithms for the fine and coarse smoothers, where ν smoothing steps have to be carried out, are presented, respectively, in Algorithm 1 and in Algorithm 2. Finally, all the ingredients introduced so far for our nonlinear multigrid

are condensed in Algorithm 3, where a single V-Cycle of the method is presented. Our nonlinear MGM iterates for $k = 0, 1, \dots, k_{\max}$, with $k_{\max} \in \mathbb{N}$, until convergence. The convergence criterion is determined by the norm of the residual of (22) where the vector components corresponding to the active dofs $i \in W^k$ are set to zero. If this norm is smaller than a given tolerance, then we stop; otherwise, we continue to the next V-Cycle.

Algorithm 1. $[\mathbf{y}_J, \mathbf{z}_J, W]$=FineSmoothing $(\mathbf{y}_J, \mathbf{z}_J, W, \mathbf{A}_J, \mathbf{f}_J, \mathbf{B}_J, \mathbf{h}_J, \mathbf{low}_J, \mathbf{up}_J, \nu)$

while $s = 1, \dots, \nu$ **do**
  while $i = 1, \dots, n_J$ **do**
    $[\mathbf{A}_{J,i}, \mathbf{B}_{J,i}, \mathbf{f}_{J,i}, \mathbf{h}_{J,i}, \mathbf{low}_{J,i}, \mathbf{up}_{J,i}]$=LocalFineProblem$(\mathbf{y}_J, \mathbf{z}_J, \mathbf{A}_J, \mathbf{B}_J, \mathbf{f}_J, \mathbf{h}_J, \mathbf{low}_J, \mathbf{up}_J)$ ▷ Compute (23), (24)
    $[\mathbf{y}_J, \mathbf{z}_J, W]$=ConstrainedMinProblem$(W, \mathbf{A}_{J,i}, \mathbf{B}_{J,i}, \mathbf{f}_{J,i}, \mathbf{h}_{J,i}, \mathbf{low}_{J,i}, \mathbf{up}_{J,i})$ ▷ Solve (27)
    $\mathbf{y}_J \leftarrow \mathbf{y}_J + \mathbf{\Pi}_{J,i}\mathbf{y}_{J,i}$
    $\mathbf{z}_J \leftarrow \mathbf{y}_J + \mathbf{\Pi}_{J,i}\mathbf{z}_{J,i}$
  end while
end while

Algorithm 2. $[\mathbf{y}_j, \mathbf{z}_j]$=CoarseSmoothing$(\mathbf{y}_j, \mathbf{z}_j, \mathbf{A}_j, \mathbf{f}_j, \mathbf{B}_j, \mathbf{h}_j, \nu)$

while $s = 1, \dots, \nu$ **do**
  while $i = 1, \dots, n_j$ **do**
    $[\mathbf{A}_{j,i}, \mathbf{B}_{j,i}, \mathbf{f}_{j,i}, \mathbf{h}_{j,i}]$=LocalCoarseProblem$(\mathbf{y}_j, \mathbf{z}_j, \mathbf{A}_j, \mathbf{B}_j, \mathbf{f}_j, \mathbf{h}_j)$ ▷ Compute (23)
    $[\mathbf{y}_j, \mathbf{z}_j]$=SolveSaddlePoint$(\mathbf{A}_{j,i}, \mathbf{B}_{j,i}, \mathbf{f}_{j,i}, \mathbf{h}_{j,i})$ ▷ Solve (28)
    $\mathbf{y}_j \leftarrow \mathbf{y}_j + \mathbf{\Pi}_{j,i}\mathbf{y}_{j,i}$
    $\mathbf{z}_j \leftarrow \mathbf{y}_j + \mathbf{\Pi}_{j,i}\mathbf{z}_{j,i}$
  end while
end while

We notice that in Algorithm 3 only the global equality constraints are projected onto the coarser levels, while the box-constraints are not. In principle, also the box-constraints could be projected by means of the monotone restriction operators, as done for the monotone MGM in References 3-5. The idea would be to define $\mathbf{low}_j$/ $\mathbf{up}_j$ on the coarser levels, for $j = 0, \dots, J-1$, so that also the coarse correction does not violate the finer constraints. The authors have tried the strategy, but the convergence is not beneficially affected and, sometimes, it is even slower. Furthermore, the fine global equality constraints $\mathbf{B}_J\mathbf{y}_J = \mathbf{h}_J$ are just projected onto the coarser levels and, thus, they already cannot be fulfilled exactly. As also observed in Reference 7, after the prolongation process, the fine smoother would take care of any violation of the box-constraints. For this reason, satisfying, exactly or in an approximate way, the box constraints is not necessary: other constraints are already not fully represented on coarser levels. Therefore, on the fine level J, we use the nonlinear smoother of Algorithm 1. On the levels, $j = 0, \dots, J-1$, we opt for Algorithm 2.

The two main ingredients of the MGM are the fine smoothing and the computation of the coarse correction. In our approach, the two are strongly interconnected and depend on the parameter α. In Section 6, we examine both the nonlinear smoother and the MGM. We will see that the value of α can influence the convergence speed of the smoother, see Figures 6 and 7. For some values of α, the convergence is better than for other values, especially for small meshes. For larger meshes, the convergence rate is smaller and is practically the same for different values of α. However, in all cases, the norm of the residual always decreases. That means that the nonlinear smoother applied on the fine level is convergent.

Nevertheless, as a smoother, its convergence rate deteriorates by increasing the dimension of the problem. That is why a MGM is needed. However, in contrast to the nonlinear smoother case, the MGM convergence is attained only for certain values of α, see Figures 8 and 9. The fact that the nonlinear smoother is convergent for different values of α, while

Algorithm 3. $[\mathbf{y}_J^{k+1}, \mathbf{z}_J^{k+1}, W^{k+1}] = \text{VCycle}\,(\mathbf{y}_J^k, \mathbf{z}_J^k, W^k, \nu_{\text{pre}}, \nu_{\text{post}})$

$[\mathbf{y}_J^k, \mathbf{z}_J^k, W^k]$=FineSmoothing$\left(\mathbf{y}_J^k, \mathbf{z}_J^k, W^k, \mathbf{A}_J, \mathbf{f}_J, \mathbf{B}_J, \mathbf{h}_J, \mathbf{low}_J, \mathbf{up}_J, \nu_{\text{pre}}\right)$ ▷ Use Algorithm 1
while $j = J-1, \dots, 0$ **do**
  if j=J-1 **then** $\hat{\mathbf{\Pi}}_j^{j+1,k}$=Truncate($\mathbf{\Pi}_j^{j+1}, W^k$) ▷ Compute (21a)
  else if $j < J-1$ **then**$\hat{\mathbf{\Pi}}_j^{j+1,k}=\mathbf{\Pi}_j^{j+1}$
  end if
  $[\mathbf{A}_j^k, \mathbf{f}_j^k, \mathbf{B}_j^k, \mathbf{h}_j^k]$=CoarseProblem$\left(\mathbf{A}_{j+1}^k, \mathbf{f}_{j+1}^k, \mathbf{B}_{j+1}^k, \mathbf{h}_{j+1}^k, \hat{\mathbf{\Pi}}_j^{j+1,k}, \mathbf{Q}_j^{j+1}\right)$ ▷ Compute (21b), (21c), (21d), (21e)
  if j > 0 **then**
    $\mathbf{y}_j^k, \mathbf{z}_j^k \leftarrow 0$
    $[\mathbf{y}_j^k, \mathbf{z}_j^k]$=CoarseSmoothing$\left(\mathbf{y}_j^k, \mathbf{z}_j^k, \mathbf{A}_j^k, \mathbf{f}_j^k, \mathbf{B}_j^k, \mathbf{h}_j^k, \nu_{\text{pre}}\right)$ ▷ Use Algorithm 2
  else if j=0 **then**
    $[\mathbf{y}_0^k, \mathbf{z}_0^k]$=Solve($\mathbf{y}_0^k, \mathbf{z}_0^k, \mathbf{A}_0^k, \mathbf{f}_0^k, \mathbf{B}_0^k, \mathbf{h}_0^k$) ▷ Solve the problem (20) for $j = 0$
  end if
end while
while $j = 0, \dots, J-2$ **do**
  $\mathbf{y}_{j+1}^k \leftarrow \mathbf{y}_{j+1}^k + \hat{\mathbf{\Pi}}_j^{j+1,k}\mathbf{y}_j^k$
  $\mathbf{z}_{j+1}^k \leftarrow \mathbf{y}_{j+1}^k + \mathbf{Q}^{j+1}\mathbf{z}_j^k$
  $[\mathbf{y}_{j+1}^k, \mathbf{z}_{j+1}^k]$=CoarseSmoothing$\left(\mathbf{y}_{j+1}^k, \mathbf{z}_{j+1}^k, \mathbf{A}_{j+1}^k, \mathbf{f}_{j+1}^k, \mathbf{B}_{j+1}^k, \mathbf{h}_{j+1}^k, \nu_{\text{post}}\right)$ ▷ Use Algorithm 2
end while
$\mathbf{y}_J^k \leftarrow \mathbf{y}_J^k + \hat{\mathbf{\Pi}}_{J-1}^{J,k}\mathbf{y}_{J-1}^k$
$\mathbf{z}_J^k \leftarrow \mathbf{y}_J^k + \mathbf{Q}_{J-1}^J\mathbf{z}_{J-1}^k$
$[\mathbf{y}_J^k, \mathbf{z}_J^k, W^k]$=FineSmoothing$\left(\mathbf{y}_J^k, \mathbf{z}_J^k, W^k, \mathbf{A}_J, \mathbf{f}_J, \mathbf{B}_J, \mathbf{h}_J, \mathbf{low}_J, \mathbf{up}_J, \nu_{\text{post}}\right)$ ▷ Use Algorithm 1
$\mathbf{y}_J^{k+1} \leftarrow \mathbf{y}_J^k$
$\mathbf{z}_J^{k+1} \leftarrow \mathbf{z}_J^k$
$W^{k+1} \leftarrow W^k$

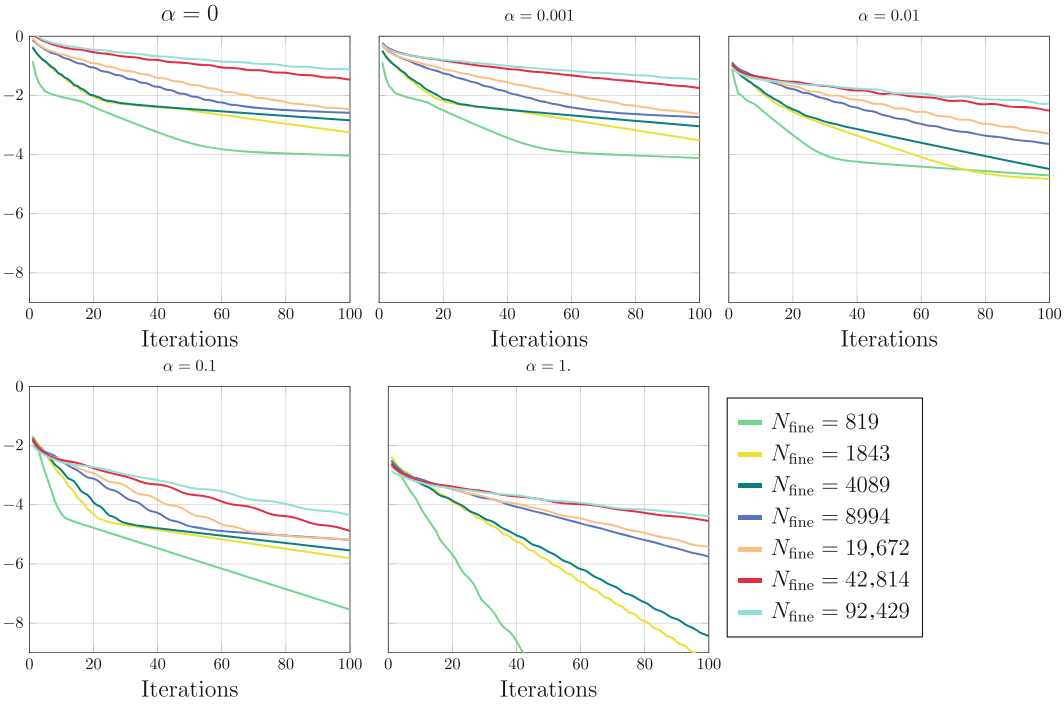

FIGURE 6 $\log_{10}$ of the Euclidean norm of the residual for the smoother method applied to the dual formulation for the Signorini problem of Figure 10 with a uniform mesh. Parameters: $\mu = 1$, $\lambda = \infty$.

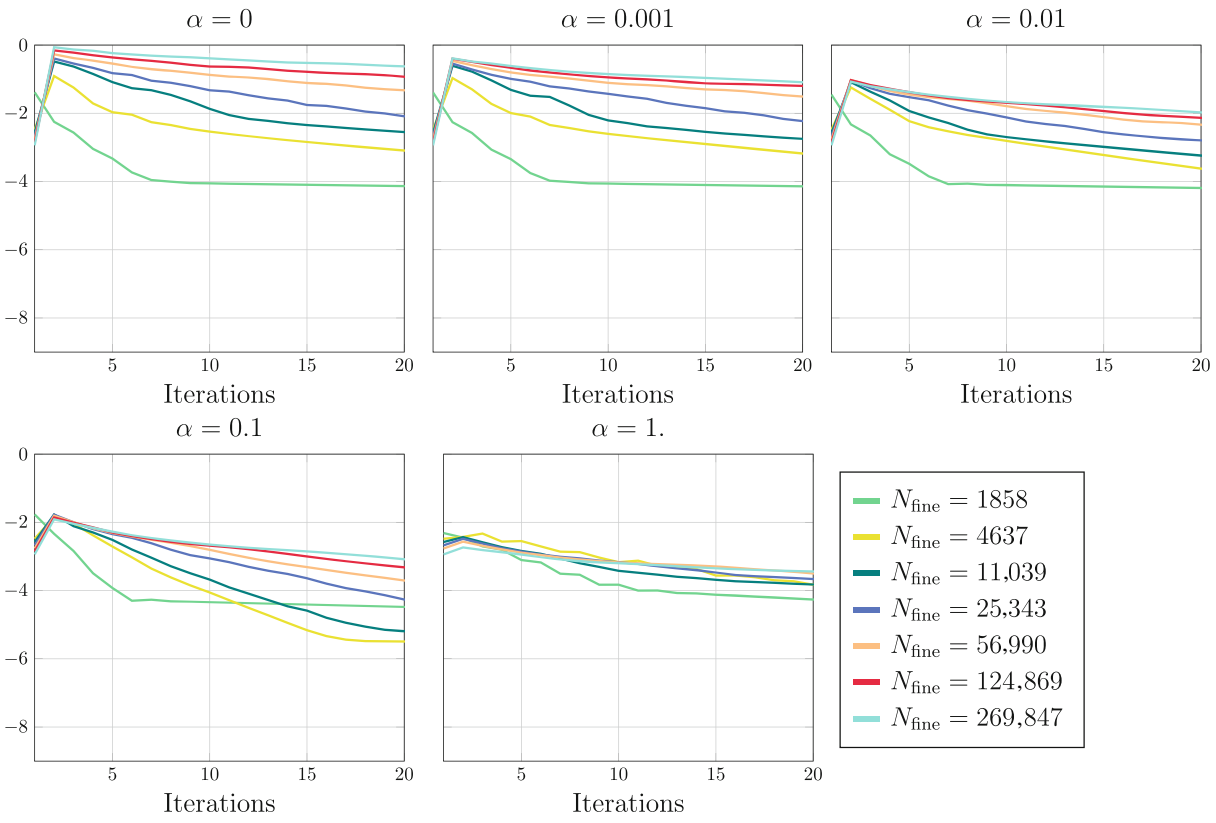

FIGURE 7 $\log_{10}$ of the Euclidean norm of the residual for the smoother method applied to the dual formulation for the Signorini problem of Figure 12 with a nonuniform mesh. Parameters: $\mu = 1$, $\lambda = \infty$.

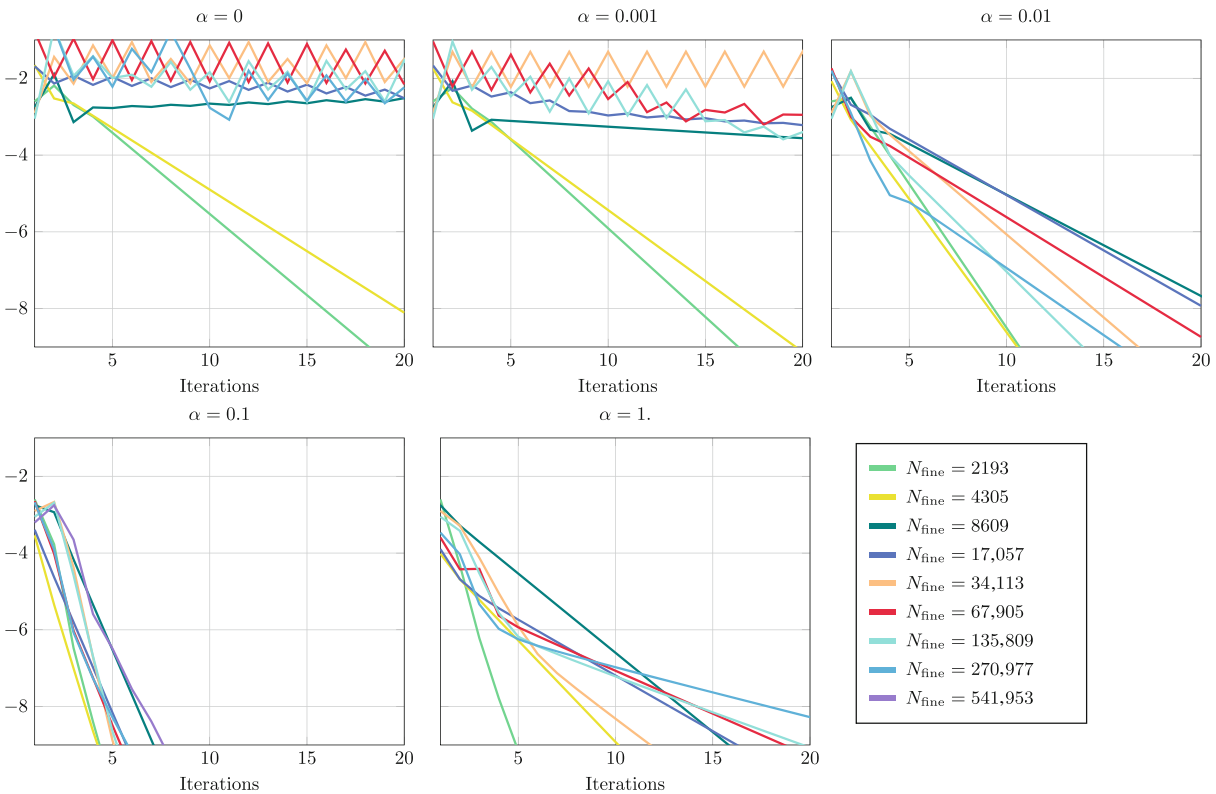

FIGURE 8 $\log_{10}$ of the Euclidean norm of the residual for the multigrid method (MGM) applied to the dual formulation for the Signorini problem of Figure 10 with a uniform mesh. Parameters: $\mu = 1$, $\lambda = \infty$, number of smoothing steps = 3. Coarse level dimension $N_{\text{coarse}} = 1097$.

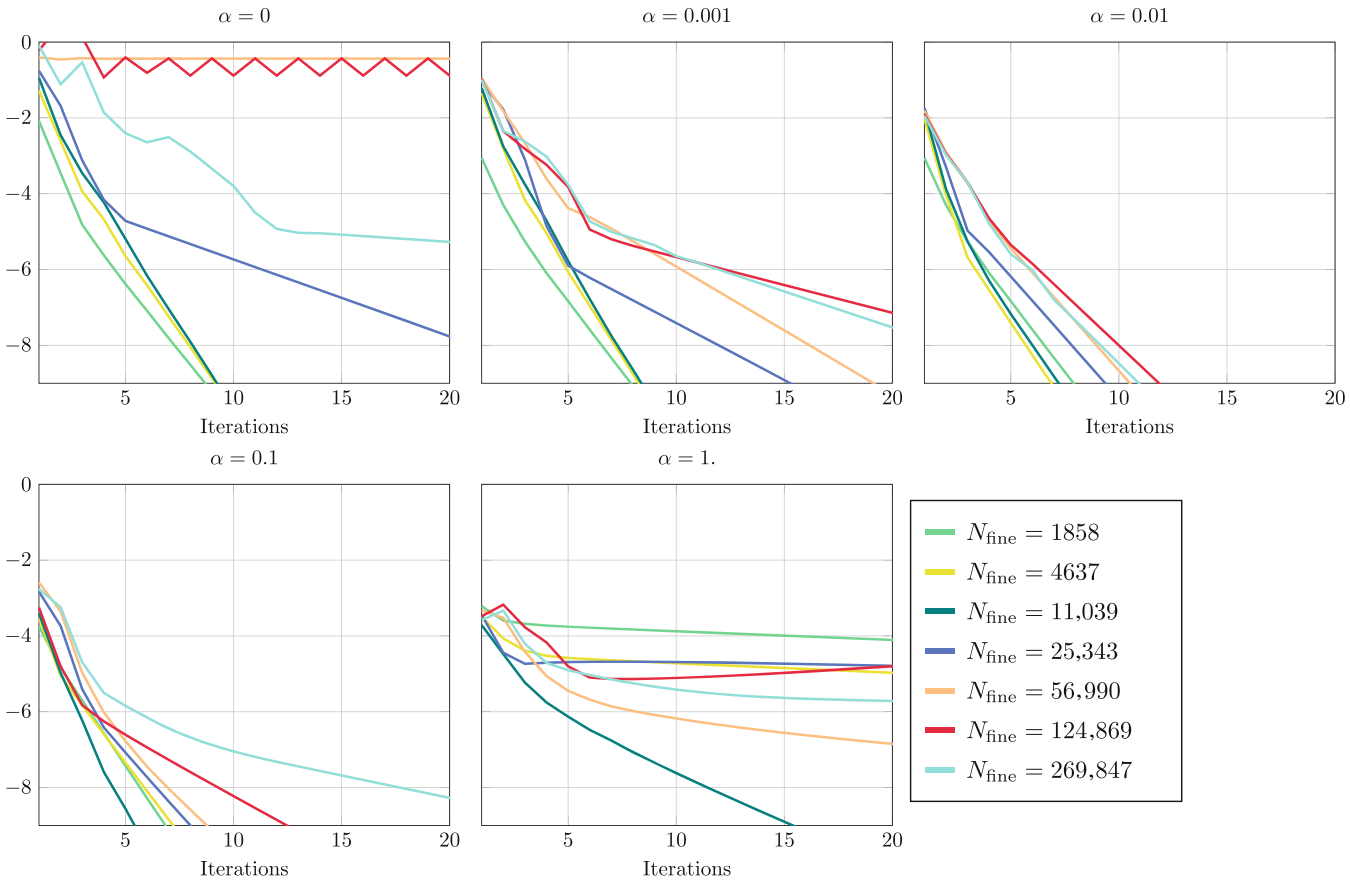

FIGURE 9 $\log_{10}$ of the Euclidean norm of the residual for the multigrid method applied to the dual formulation for the Signorini problem of Figure 12. Parameters: $\mu = 1$, $\lambda = \infty$, number of smoothing steps = 3. Coarse level dimension $N_{\text{coarse}} = 579$.

the MGM is not, suggests that a working smoother is not enough. As it is well known from the multigrid literature, the entire MGM process must be examined by studying all together, the smoothing and the coarsening.

We have already investigated this kind of behavior for a two-grid method applied to the linear elastic case. In Reference 12, we compute an exact coarse correction, so that it is the same for any value of α. In this way, the process is influenced by α only at the fine level. The addition of the coarse correction ensures global communication that only the fine smoother cannot guarantee. Thus, its computation is still fundamental, as for all MGMs. So, it is clear that the overall convergence behavior of the MGM depends on how the fine smoothing steps act on the current solution after the addition of the interpolated coarse correction.

From the experiments, it is evident that the parameter α plays an important role. In the linear case, convergence can be always attained, but the speed depends heavily on α. In the nonlinear case, the choice of α is not only relevant for the convergence speed, but also for the convergence itself. This is because the fine smoothing must not only smooth the high-frequency components of the error but also take care of the constraints. Thus, it is not sufficient to study the smoother as a stand-alone solver. The multigrid process has to be examined as a whole and even more so in the Signorini case.

In conclusion, the parameter α used for the smoother on the fine level has a direct impact also on what happens on the coarser levels, due to the presence of constraints. It does not only govern the communication among the patches, but it is also important for ensuring the admissibility of the iterate with respect to the global constraints.

6 | NUMERICAL EXPERIMENTS

In this section, we examine both our nonlinear smoother on the fine level and MGM for a convex and a nonconvex domains, respectively in Sections 6.1 and 6.2. We repeat the experiments for different values of α.

6.1 | Uniform square mesh against circular obstacle

Let $\Omega = [0,1] \times [0,1]$ be a square domain, with $\mu = 1$ and $\lambda = \infty$. On the left and right edges, we enforce free Neumann boundary conditions: $\mathbf{g}_N|_{\text{left}} = \mathbf{g}_N|_{\text{right}} = [0,0]^T$. On the bottom, we set a uniform vertical displacement $\mathbf{g}_D|_{\text{bottom}} = [0, 0.01]^T$. The top side is the contact boundary Γ_C. The obstacle is described by a semicircle of center $\mathbf{c} = [0.5, 1.5]^T$ and radius $r = 0.5$. See Figure 10. We have tested our nonlinear smoother at the fine level and our nonlinear MGM with different values of $\alpha \in [0,1]$. However, we discuss the most representative ones: $\alpha = 0,\ 0.001,\ 0.01,\ 0.1,\ 1$. Parameters $\alpha > 1$ make the MGM method divergent. This can happen even for the linear case, see the numerical experiments in Reference 12.

We consider the coarsest uniform square mesh $\mathcal{T}_0$ to be the one corresponding to $N_{\text{coarse}} = 1097$ dofs. We sequentially refine it, by means of a bisection algorithm. We get the hierarchy of nested meshes $\{\mathcal{T}_j\}_{j=0}^{9}$. Then we examine the MGM for different fine leves $J = 1, \ldots, 9$, where level $J = 9$ corresponds to $N_{\text{fine}} = 541{,}953$. We set $\nu_{\text{pre}} = \nu_{\text{post}} = 3$. So we do three presmoothing steps and three postsmoothing steps at each level, except for the coarsest one, where an exact solver is used. Solutions of the problem can be found in Figure 11. The convergence results are represented in Figure 8. The convergence is optimal for $\alpha = 0.1$, since it does not depend on the number of levels and the number of dofs. At least among the values used, we can state $\alpha_{\text{opt}} = 0.1$. The more α is chosen far away from this value, the more iterations are required for the MGM to converge, and the more the number of levels has an important effect. Furthermore, if α is too far away, then the method can even not converge. In particular, it is interesting to notice that for too small values of α, for example, $\alpha \in [0, 0,\ 0.001]$, and for sufficiently fine meshes, the MGM does not converge. Thus, in contrast to the linear case, where $\alpha = 0$ for a multilevel strategy could be chosen with no problem, now the local Robin conditions are fundamental for the convergence of the method.

6.2 | Square mesh with hole against two circular obstacles with different radii

We consider a square domain $\Omega = [0,1] \times [0,1]$, with a square hole $[0.25, 0.75] \times [0.25, 0.75]$. The Lamé parameters of the body are $\mu = 1$ and $\lambda = \infty$. The contact boundary Γ_C consist of the top external and the bottom internal edges. The two circular rigid obstacles have, respectively, centers $\mathbf{c}_1 = [0.75, 1.5]^T$ and $\mathbf{c}_2 = [3/8, 5/12]^T$, and radii $r = 0.5$ and $r = 1/6$. On the bottom external edge, we enforce a uniform vertical displacement $\mathbf{g}_D|_{\text{bottom}} = [0, 0.01]^T$. On the rest of $\partial\Omega$, we set free Neumann boundary conditions. See Figure 12 for the setting and Figure 13 for the solution of the problem.

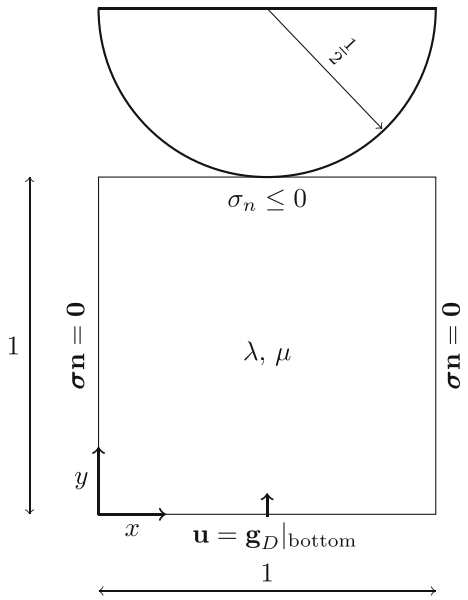

FIGURE 10 One body contact problem with rigid body obstacle.

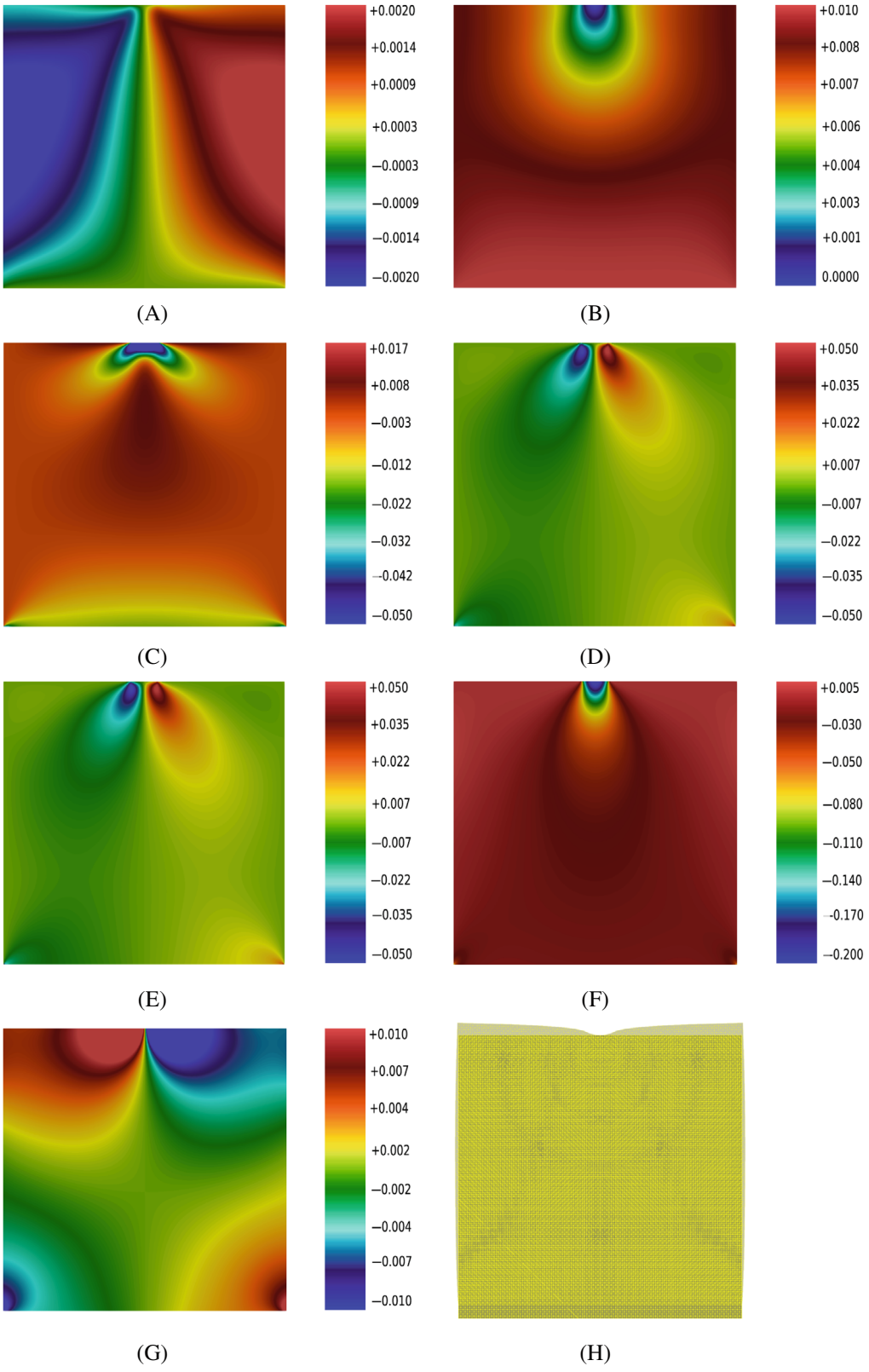

FIGURE 11 Results for the problem in Figure 10 with a uniform mesh. Parameters: $\mu = 1$, $\lambda = \infty$. (A) u_x; (B) u_y; (C) σ_{xx}; (D) σ_{xy}; (E) σ_{yx}; (F) σ_{yy}; (G) ρ; (H) five times deformed mesh.

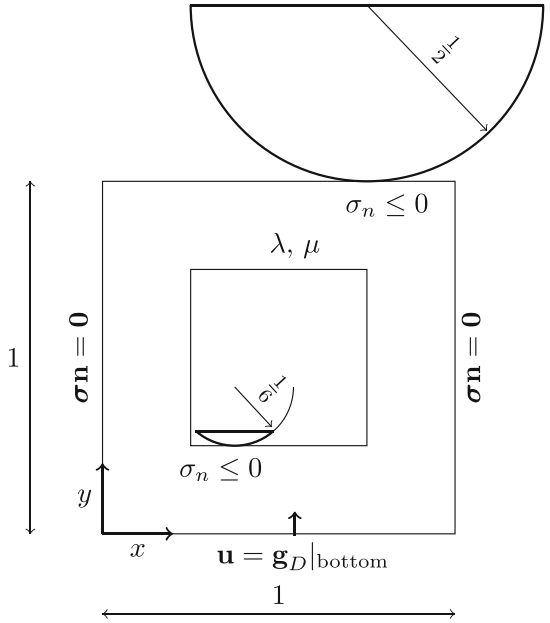

FIGURE 12 Nonconvex body with a hole in contact with two rigid body obstacles. Contact boundaries are fixed to be the top external and the bottom internal edges. There, both $\sigma_n \leq 0$ and $\boldsymbol{\sigma}\boldsymbol{n} - \sigma_n\boldsymbol{n} = \mathbf{0}$ hold. On the bottom external edge a uniform vertical displacement is enforced, that is, $\mathbf{g}_D|_{\text{bottom}} = [0, 0.01]^T$. Everywhere else, free Neumann boundary conditions $\boldsymbol{\sigma}\boldsymbol{n} = \mathbf{0}$ are imposed.

We consider a coarse mesh of $N_{\text{coarse}} = 579$ dofs. The coarse mesh is already created so that it is more refined in the neighborhood of the two obstacles. In this way, we do not require any adaptive-mesh refinement and we can use a bisection algorithm as for the previous example.

We again use $\nu_{\text{pre}} = \nu_{\text{post}} = 3$. We examine the MGM for varying values of $\alpha = 0,\ 0.001,\ 0.01,\ 0.1,\ 1$. From Figure 9, we can state that $\alpha_{\text{opt}} = 0.01$ make the MGM optimal. Furthermore, the behavior of the MGM is more sensitive to the choice of α. We can guess that the more complex is the problem, the more α has to be chosen carefully.

6.3 | Dynamic reduction of α

The choice of the parameter $\alpha \geq 0$ has a very important influence on the convergence of the MGM and depends on the specific problem. We know that α cannot be too large or too small, that is, $\alpha \in (0, 1]$. Furthermore, we know that the closer α is to α_{opt}, the better the convergence. Thus, we can define the "number of iterations" as a function of α. Experimentally, we can see that this function has a global minimum $\alpha_{\text{opt}} \in [0, 1]$, decreases in $[0, \alpha_{\text{opt}}]$ and increases in $\alpha \in [\alpha_{\text{opt}}, 1]$. See Figure 14. We do propose a dynamic strategy that is based on this assumption.

Given an initial value $\alpha_0 \in (0, 1]$, at each kth V-Cycle, we update the value α_k. For simplicity, we have decided to make α belong to a countable set A, defined as follows:

$$A := \{25 \cdot 10^{-k}, 50 \cdot 10^{-k}, 75 \cdot 10^{-k}, 100 \cdot 10^{-k}, \quad k \in \mathbb{N}\}. \tag{29}$$

The initial value for α is $\alpha_0 \in A$. Then, at the iteration $k \geq 0$, given $\alpha_k \in A$, we need to find $\alpha_{k+1} \in A$. We define $r_k = \log_{10} \|\mathbf{r}_k\|$, where $\mathbf{r}_k$ is the residual of (22) at the kth iteration, with $[\mathbf{r}_k]_i = 0$ for $i \in W^k$. If the kth residual decrease is large enough, the same value for α is kept and thus $\alpha_{k+1} = \alpha_k$. This happens if $r_k - r_{k-1} < -\eta$, where η is a positive number that we choose to be $\eta = 0.6$. Otherwise we decrease the value:

$$\alpha_{k+1} = \text{argmax}\{\alpha \in A : \alpha < \alpha_k\}. \tag{30}$$

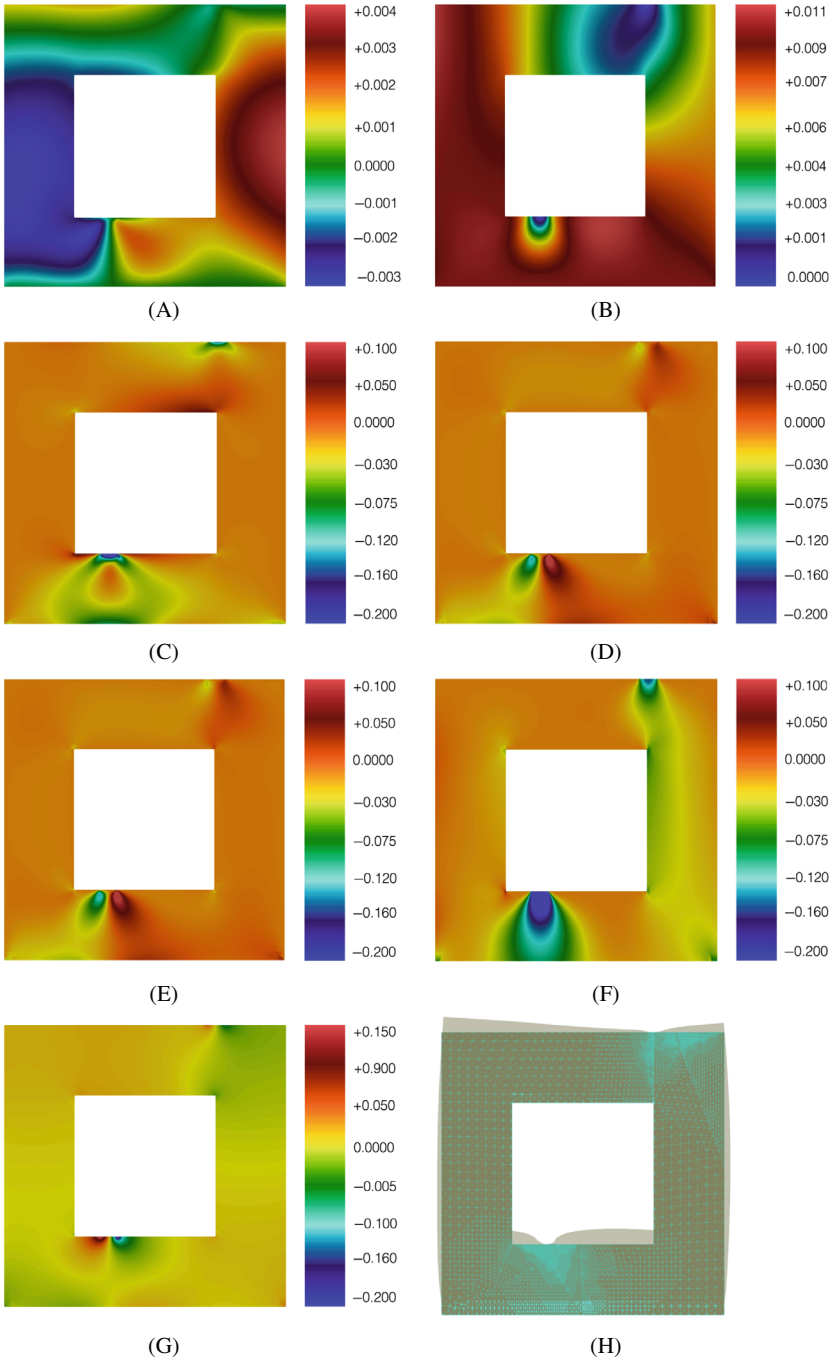

FIGURE 13 Results for the problem of Figure 12. Parameters: $\mu = 1$, $\lambda = \infty$. (A) u_x; (B) u_y; (C) σ_{xx}; (D) σ_{xy}; (E) σ_{yx}; (F) σ_{yy}; (G) ρ; (H) deformed mesh.

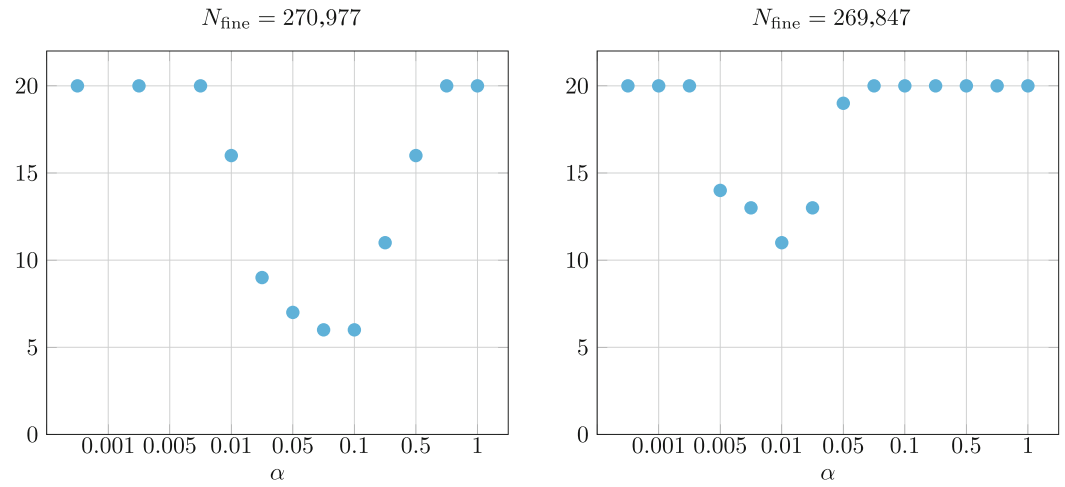

FIGURE 14 Number of multigrid method iterations, with a maximum of 20 iterations, against α. Left: problem of Figure 10. Right: problem of Figure 12.

The whole process is described in Algorithm 4. Given $\eta = 0.6$, results for Algorithm 4 can be found in Figure 15. We have considered the cases with the smallest and the largest fine meshes. In the row related to α, we see that, if N_{fine} is small enough, α is almost unchanged. On the other hand, for larger meshes, the method is more sensitive to the value of α_0. However, we see that fast convergence is obtained in all cases if the value α_0 is such that $\alpha_0 \geq \alpha_{\text{opt}}$ and if it is not too large. If $\alpha_0 \ll \alpha_{\text{opt}}$, no convergence is attained. Furthermore, the number of iterations to get convergence is almost the same for the smallest or the largest fine mesh.

This means that Algorithm 4 makes the MGM optimal, that is dimension and level independent, if $\alpha_0 \in [\alpha_{\text{opt}}, 1]$.

If at first, it was necessary to determine from the beginning a value α sufficiently close to α_{opt}, now with Algorithm 4 it is sufficient to choose it in a larger range of values, $\alpha_0 \in [\alpha_{\text{opt}}, 1]$. The combination of Algorithm 4 and the MGM method, if $\alpha_0 \in [\alpha_{\text{opt}}, 1]$, gives rise to multigrid performance for the dual weak form of the Signorini problem in the nearly incompressible and incompressible cases.

Remark 5. The set A is arbitrary and we can define it with many more values for a given k. Furthermore, the number of values could vary for varying k. For example, we could increase the number of values for increasing of the parameter k, so that the research of α_{opt} becomes more and more accurate.

Remark 6. We have tried many other different strategies for updating α. We can mention the most important ones in this remark. The first one is to optimize α on a each patch. However, it is not possible to compute α on each patch independently from the other patches. The role of α is to enhance the global communication process among the patches and this can be done only if α is the same for a whole smoothing process. Thus, another strategy could be to update α_k between different smoothing steps or V-Cycles. For example, we could increase or decrease the value of α_k. Even though this strategy is admissible, it is unstable and it depends too much on the problem and on the initial value α_0. A monotone reduction of α_k is the simplest but also the most effective strategy that we have examined.

Algorithm 4. α_{k+1}=AlphaReduction(η, r_k, r_{k-1}, α_k, A)

if $r_k - r_{k-1} < -\eta$ **then** $\alpha_{k+1} \leftarrow \alpha_k$
else $\alpha_{k+1} \leftarrow \text{argmax}\{\alpha \in A : \alpha < \alpha_k\}$
end if

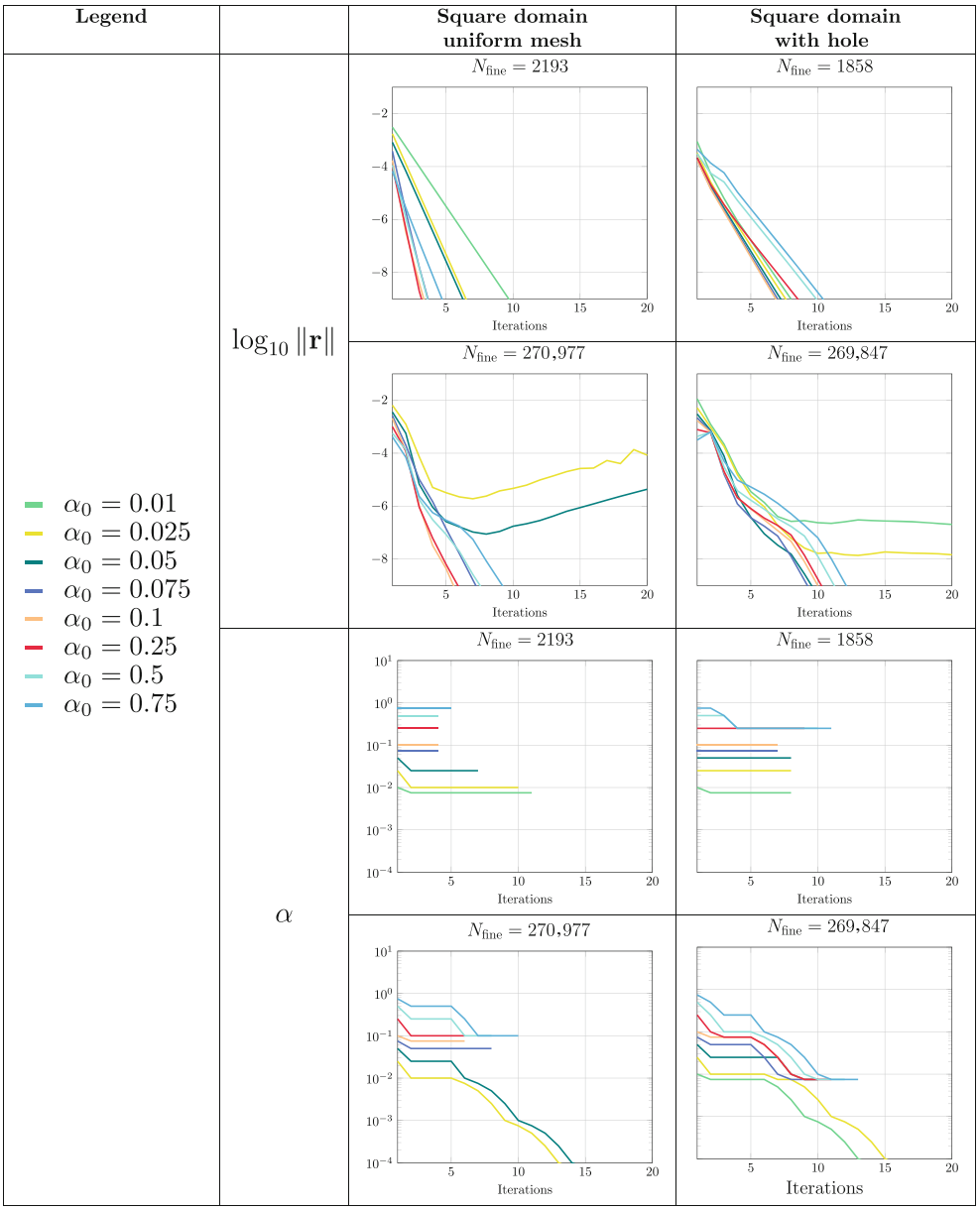

FIGURE 15 Results related to Algorithm 4.

7 | CONCLUSION

In this paper, we have designed an optimal nonlinear MGM for the dual Signorini problem for nearly incompressible and incompressible materials, discretized by means of the FE method. A linear MGM for the dual problem of linear elasticity has been proposed in Reference 12, where a monolithic patch smoother with local Robin boundary conditions of parameter α is used. With respect to the linear elastic case, the main difference of the dual Signorini problem resides in the negativity of the pressure condition, that is, $\sigma_n \leq 0$. In the FE setting, if local Householder transformations are exploited, such nonlinearity reduces to box-constraints. In order to maintain the overall optimality, the box-constraints must be tackled on the fine and on the coarser levels. On the fine level, we do so by using a nonlinear smoother that solves for constrained optimization problems on patches where Robin conditions are imposed. On coarser levels, we transfer the fine information of the momentary active set by means of the truncation of the basis functions strategy. Numerical experiments show that our MGM is optimal for certain values of α. However, the optimal value α_{opt} is not known a priori. For this reason, we do also propose an algorithm for its dynamic update at every kth V-Cycle. If the initial value $\alpha_0 \in [\alpha_{\text{opt}}, 1]$, then our MGM method, for the dual Signorini problem for nearly incompressible and incompressible

materials, exhibits an optimal convergence rate. Future works on this topic should try to come up with a more general strategy to determine α. Nevertheless, the authors are confident that this paper could help the scientific community in this purpose.

ACKNOWLEDGMENTS

The authors would like to thank the Swiss National Science Foundation for their support through the project and the Deutsche Forschungsgemeinschaft (DFG) for their support in the SPP 1962 "Stress-Based Methods for Variational Inequalities in Solid Mechanics: Finite Element Discretization and Solution by Hierarchical Optimization (186407)". Open access funding provided by Universita della Svizzera italiana.

CONFLICT OF INTEREST STATEMENT

The authors declare no potential conflict of interests.

DATA AVAILABILITY STATEMENT

The data that support the findings of this study are openly available in rovi_dual_signorini_multigrid at https://bitbucket.org/Garo91/rovi_dual_signorini_multigrid/src/master/.

REFERENCES

1. Kikuchi N, Oden JT. *Contact Problems in Elasticity: A Study of Variational Inequalities and Finite Element Methods*. Vol 8. SIAM; 1988.
2. Brezzi F, Fortin M. *Mixed and Hybrid Finite Element Methods*. Vol 15. Springer Science & Business Media; 2012.
3. Kornhuber R. Monotone multigrid methods for elliptic variational inequalities I. *Num Math*. 1994;69(2):167-184.
4. Kornhuber R. Monotone multigrid methods for elliptic variational inequalities II. *Num Math*. 1996;72(4):481-499.
5. Kornhuber R, Krause R. Adaptive multigrid methods for Signorini's problem in linear elasticity. *Comput Visual Sci*. 2001;4(1):9-20.
6. Kornhuber R, Krause R, Sander O, Deuflhard P, Ertel S. A monotone multigrid solver for two body contact problems in biomechanics. *Comput Visual Sci*. 2008;11(1):3-15.
7. Krause R. A nonsmooth multiscale method for solving frictional two-body contact problems in 2D and 3D with multigrid efficiency. *SIAM J Sci Comput*. 2009;31(2):1399-1423.
8. Krause R, Rigazzi A, Steiner J. A parallel multigrid method for constrained minimization problems and its application to friction, contact, and obstacle problems. *Comput Visual Sci*. 2016;18(1):1-15.
9. Badea L. *Convergence Rate of a Multiplicative Schwarz Method for Strongly Nonlinear Variational Inequalities*. Springer; 2002:31-41.
10. Badea L. Global convergence rate of a standard multigrid method for variational inequalities. *IMA J Num Anal*. 2014;34(1):197-216.
11. Badea L, Krause R. One-and two-level Schwarz methods for variational inequalities of the second kind and their application to frictional contact. *Num Math*. 2012;120(4):573-599.
12. Rovi G, Krause R. Patch-smoother and multigrid for the dual formulation for linear elasticity. *Int J Num Methods Eng*. 2021;122(24):7609-7631.
13. Kober B. *Stress-based Finite Element Methods for Variational Inequalities in Contact Mechanics*. Universität Duisburg-Essen; 2020.
14. Rognes ME, Kirby RC, Logg A. Efficient assembly of H(div) and H(curl) conforming finite elements. *SIAM J Sci Comput*. 2009;31(6):4130-4151.
15. Xu J. Iterative methods by space decomposition and subspace correction. *SIAM Rev*. 1992;34(4):581-613.
16. Bank RE, Yserentant H. Multigrid convergence: a brief trip down memory lane. *Comput Visual Sci*. 2010;13(4):147-152.
17. Xu J. The auxiliary space method and optimal multigrid preconditioning techniques for unstructured grids. *Computing*. 1996;56(3):215-235.
18. Chen Z. *Multigrid Algorithms for Mixed Methods for Second Order Elliptic Problems*. IMA; 1994.
19. Gelman E, Mandel J. On multilevel iterative methods for optimization problems. *Math Program*. 1990;48(1-3):1-17.
20. Mandel J. A multilevel iterative method for symmetric, positive definite linear complementarity problems. *Appl Math Optimiz*. 1984;11(1):77-95.
21. Arnold DN, Falk RS, Winther R. Preconditioning in H(div) and applications. *Math Comput Am Math Soc*. 1997;66(219):957-984.
22. Arnold DN, Falk RS, Winther R. Multigrid in H(div) and H(curl). *Num Math*. 2000;85(2):197-217.
23. Arnold DN, Falk RS, Winther R. Multigrid preconditioning in H(div) on non-convex polygons. *Comput Appl Math*. 1998;17:303-316.

How to cite this article: Rovi G, Kober B, Starke G, Krause R. Multigrid for the dual formulation of the frictionless Signorini problem. *Int J Numer Methods Eng*. 2023;124(10):2367-2388. doi: 10.1002/nme.7214